X-ray & Neutron Scattering Studies of Microscopic Dynamics in Glasses

Jaydeep Basu
Department of Physics
Indian Institute of Science
Bangalore

International School on Glass Formers & Glasses, Jan 2010, Bangalore

Lecture Plan - Day 2

- X-ray & Neutron Scattering - Basics
- Inelastic scattering
- Time and Frequency domain measurements
- Inelastic X-ray Scattering (**Frequency domain** – High Q, High Energy)
- X-ray Photon Correlation Spectroscopy (**Time Domain** – Intermediate Q, Low Energy)
- Inelastic Neutron Scattering including Backscattering Spectroscopy (High Q and High Energy, Coherent and Incoherent Scattering - **Frequency domain**)
- Neutron Spin Echo Spectroscopy (NSE) (Low Energy, High Q , Coherent Scattering and Incoherent Scattering - **Time Domain**)

X-ray & Neutron Scattering - Basics

- X-rays interact with the charge in atoms as well as with the magnetic moment
- Neutrons interact with atomic nuclei as well as with the magnetic moment due to spins of unpaired electrons

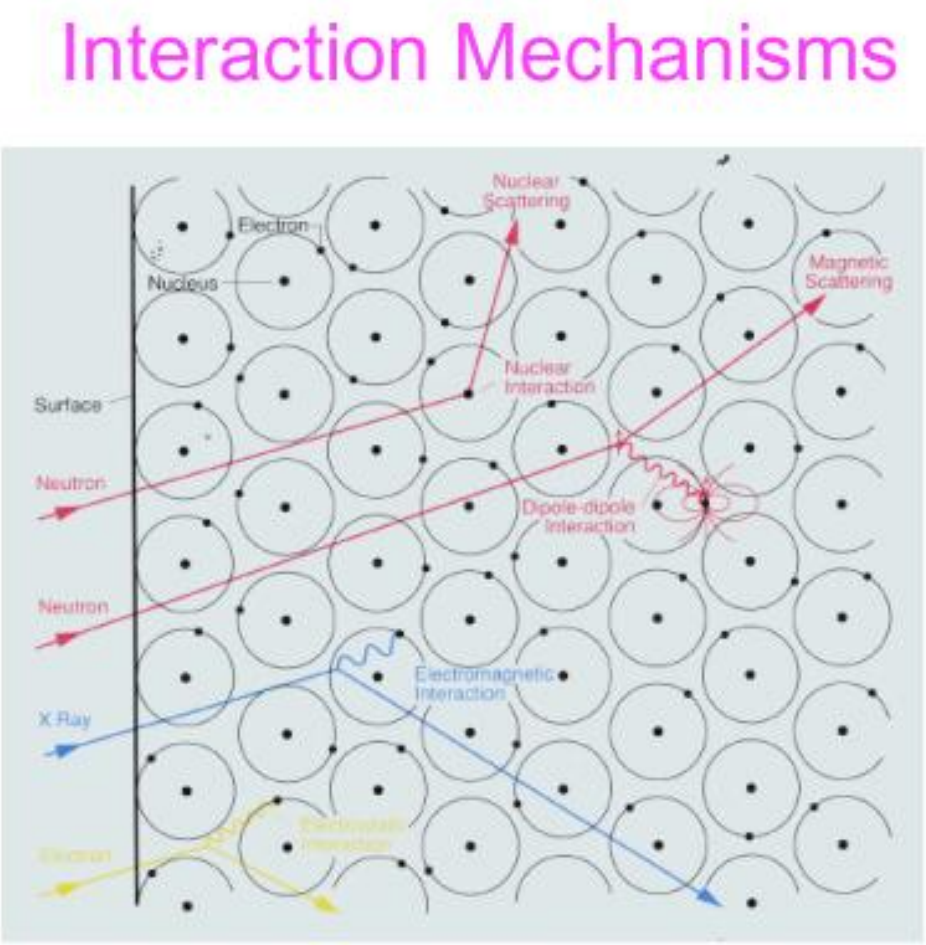

Acknowledgements

- Sunny Sinha (UCSD)
- Larry Lurio (NIU)

Properties of Neutrons

The Neutron has Both Particle-Like and Wave-Like Properties

- Mass: $m_n = 1.675 \times 10^{-27}$ kg
- Charge = 0; Spin = ½
- Magnetic dipole moment: $\mu_n = -1.913\ \mu_N$
- Nuclear magneton: $\mu_N = eh/4\pi m_p = 5.051 \times 10^{-27}$ J T^{-1}
- Velocity (v), kinetic energy (E), wavevector (k), wavelength (λ), temperature (T).
- $E = m_n v^2/2 = k_B T = (hk/2\pi)^2/2m_n$; $k = 2\pi/\lambda = m_n v/(h/2\pi)$

	Energy (meV)	Temp (K)	Wavelength (nm)
Cold	**0.1 – 10**	**1 – 120**	**0.4 – 3**
Thermal	**5 – 100**	**60 – 1000**	**0.1 – 0.4**
Hot	**100 – 500**	**1000 – 6000**	**0.04 – 0.1**

λ (nm) = 395.6 / v (m/s)
E (meV) = 0.02072 k^2 (k in nm^{-1})

Properties of X-rays

$E = h\nu = hc/\lambda = hck$

Charge = 0 Magnetic Moment = 0

Spin = 1

E (keV)	λ (Å)
0.8	15.0
8.0	1.5
40.0	0.3
100.0	0.125

Synchrotron & Neutron Sources in the World

Scattering Cross-Sections

Intrinsic Cross Section: Neutrons

$$\left(\frac{d\sigma}{d\Omega}\right)_0 = |b|^2 = \text{const.}$$

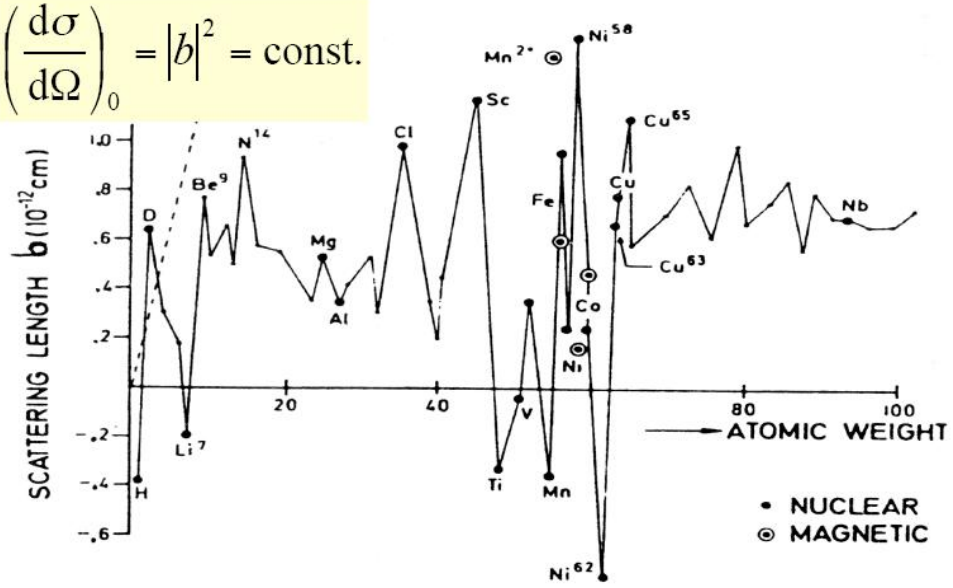

Intrinsic Cross Section: X-Rays

$$\vec{E}_{\text{in}} = \vec{E}_0 e^{i(\vec{k}\cdot\vec{r}-\omega t)}$$

$$E_{\text{rad}}(R,t) = \frac{e}{4\pi\varepsilon_0 c^2 R}\ddot{x}(t-R/c)$$

$$\ddot{x}(t-R/c) = -\frac{e}{m}\alpha(\omega)E_{\text{in}}e^{i\omega R/c}\cos\psi$$

$$\frac{E_{\text{rad}}(R,t)}{E_{\text{in}}} = -r_0\alpha(\omega)\frac{e^{ikR}}{R}\cos\psi$$

Thomson Scattering Length of the Electron (classical electron radius):

$$r_0 = \frac{e^2}{4\pi\varepsilon_0 mc^2} = 2.82\times10^{-15}\,\text{m}$$

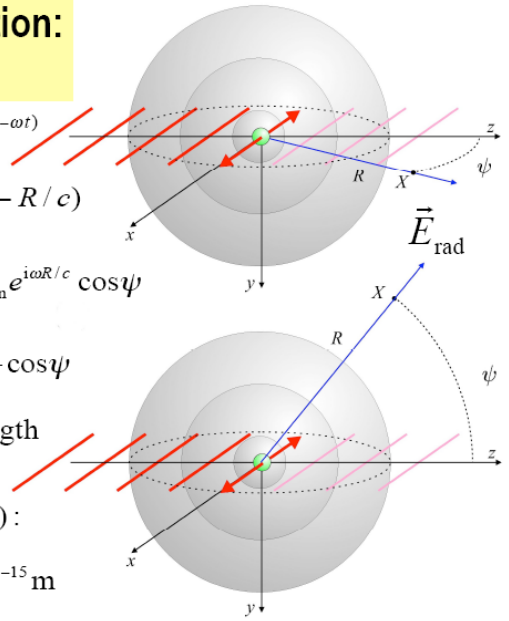

Scattering of X-rays & Neutrons

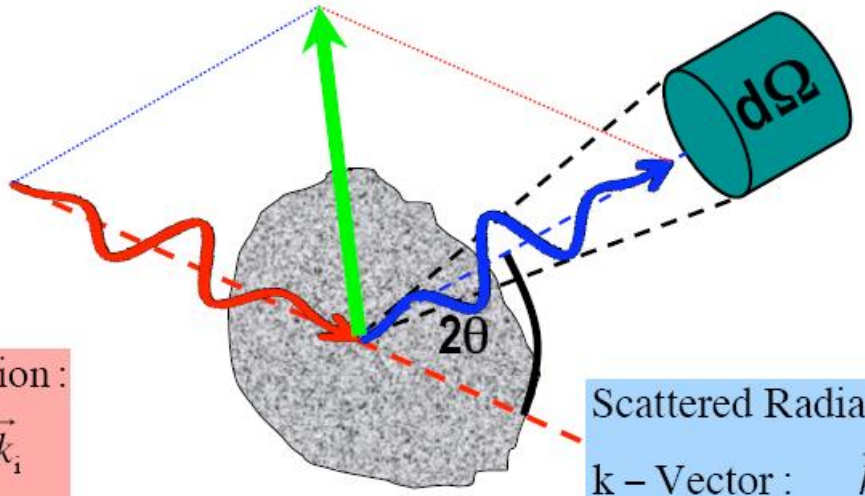

Incident Radiation :

k – Vector : $\vec{k}_i$

$|\vec{k}_i| = 2\pi/\lambda$

Energy : E_i

Polarization : $\vec{p}_i$

Scattered Radiation :

k – Vector : $\vec{k}_f$

Energy : E_f

Polarization : $\vec{p}_f$

Wavevector Transfer :

$\vec{q} = \vec{k}_f - \vec{k}_i$

Energy Transfer :

$\Delta E = E_f - E_i = \hbar\omega$

Polarization :

$\vec{p}_i \rightarrow \vec{p}_f$

For X - Rays :

$\Delta E << E_f, E_i$

$\Rightarrow \quad |\vec{q}| = 2k_i \sin(2\theta/2)$

Scattering Cross-Sections

Neutrons

Sum of scattered waves on plane II:

$$\psi_{se} = Ae^{i\phi}\sum_i \frac{b_i}{R} e^{-i\bar{q}\cdot\bar{R}_i}$$

$$\frac{d\sigma}{d\Omega} = \frac{vdS|\psi_{se}|^2}{v|A|^2\, d\Omega} = \frac{vdS}{v|A|^2}\frac{|A|^2}{R^2}\frac{1}{d\Omega}\sum_{ij} b_i b_j\, e^{-i\bar{q}\cdot(\bar{R}_i-\bar{R}_j)}$$

$$= \sum_{ij} b_i b_j\, e^{-i\bar{q}\cdot(\bar{R}_i-\bar{R}_j)}$$

X-rays

$$\frac{d\sigma}{d\Omega} = r_0^2 \sum_{ij} e^{-i\bar{q}\cdot(\bar{r}_i-\bar{r}_j)} \times \left(\frac{1+\mathrm{Cos}^2(2\theta)}{2}\right)$$

$\bar{r}_i \rightarrow$ electron coordinates

Scattering Cross-Sections

For neutrons, b_i depends on nucleus (isotope, spin relative to neutron ($\uparrow\uparrow$ or $\downarrow\uparrow$)), etc. Even for one type of atom,

$b_i = \langle b \rangle + \delta b_i$ ← random variable

$$b_i b_j = \langle b \rangle^2 + \langle b \rangle \left[\delta b_i + \delta b_j \right] + \delta b_i \, \delta b_j$$

(δb_i: zero; $\delta b_i \, \delta b_j$: zero unless $i = j$)

$$\left\langle \delta b_i^2 \right\rangle = \left\langle b^2 \right\rangle - \langle b \rangle^2$$

$$\therefore \frac{d\sigma}{d\Omega} = \langle b \rangle^2 \sum_{ij} e^{-i\vec{q}\cdot\left(\vec{R}_i - \vec{R}_j\right)} + \left[\left\langle b^2 \right\rangle - \langle b \rangle^2 \right] N$$

$\sigma_{coh}/4\pi$ "coherent" $\qquad$ $\sigma_{inc}/4\pi$ "incoherent"

In most cases, we must do a thermodynamic or ensemble average

$$\frac{d\sigma}{d\Omega} = \langle b \rangle^2 S(q) \qquad S(q) = \left\langle \sum_{ij} e^{-i\vec{q}\cdot\left(\vec{R}_i - \vec{R}_j\right)} \right\rangle$$

$\{R_i\}$ = nuclear posns

Coherent Part

Now, $\rho N(r)$ is the nuclear (basically atomic) number density

$$\rho_N(\mathbf{r}) = \Sigma_i \, \delta(\mathbf{r} - \mathbf{R_i})$$

$$\rho_N(\mathbf{q}) = \int \rho_N(\mathbf{r}) \exp[-i\mathbf{q}.\mathbf{r}] \, d\mathbf{r} = \int \Sigma_i \, \delta(\mathbf{r} - \mathbf{R_i}) \exp[-i\mathbf{q}.\mathbf{r}] \, d\mathbf{r}$$

$$= \Sigma_i \exp[-i\mathbf{q}.\mathbf{R_i}]$$

So, the structure factor S(q) can be defined as

$$S(\mathbf{q}) = \langle \rho_N(\mathbf{q}) \, \rho_N^*(\mathbf{q}) \rangle$$

For Neutrons and

$$S(\mathbf{q}) = \langle \rho_{el}(\mathbf{q}) \, \rho_{el}^*(\mathbf{q}) \rangle$$

For X-rays

$$S(q) = \left\langle |\rho_N(\bar{q})|^2 \right\rangle \qquad \left[\times |f(q)|^2\right] \text{for x-rays}$$

$$\rho_N(\bar{q}) = \int d\bar{r}\, e^{-i\bar{q}\cdot\bar{r}} \rho_N(\bar{r})$$

$$\Rightarrow S(q) = \iint d\bar{r}\, d\bar{r}'\, e^{-i\bar{q}\cdot(\bar{r}-\bar{r}')} \langle \rho_N(r)\rho_N(r') \rangle$$

If $\langle \rho_N(\bar{r})\rho_N(r') \rangle$ = Fn. of $(r - r')$ only,

$$S(q) = V \int d\bar{r}'\, e^{-i\bar{q}\cdot\bar{R}} \langle \rho_N(\bar{r})\rho_N(\bar{r}-\bar{R}) \rangle$$

$$= \int d\bar{R}\, e^{-i\bar{q}\cdot\bar{R}} g(\bar{R})$$

$g(\bar{R})$ = Pair-distribution function

$$= V \langle \rho_N(\bar{r})\rho_N(\bar{r}-\bar{R}) \rangle$$

$\Rightarrow$ Probability that given a particle at $\bar{r}$, there is distance $\bar{R}$ from it (per unit volume)

$$g(\bar{R}) = \delta(\bar{R}) + g_d(\bar{R}) \qquad S(q) - 1 = \int d\bar{R}\, e^{-i\bar{q}\cdot R} g_d(\bar{R})$$

$$g_d(\bar{R})_{R\to\infty} \to V\langle\rho\rangle^2$$

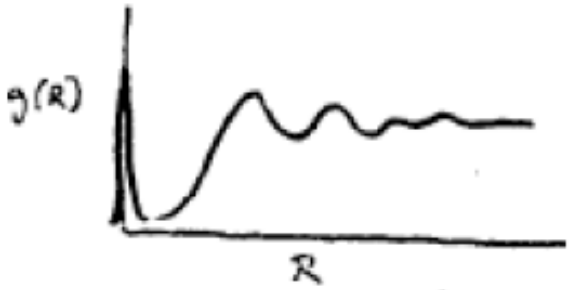

Liquids and Glasses

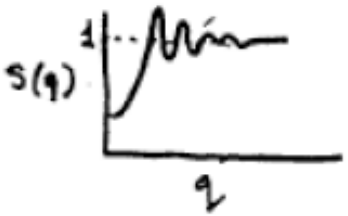

$g(\bar{R})$ and hence $S(q)$ are isotropic.

$g_d(R)$ = Reverse F.T. of $[S(q) - 1]$

$$= 4\pi \int_0^\infty dq\, q^2 \frac{\mathrm{Sin}(qR)}{(qR)} [S(q) - 1]$$

Inelastic Scattering Cross-Section

Recall that $\left(\frac{d^2\sigma}{d\Omega.dE}\right)_{coh} = b_{coh}^2 \frac{k'}{k} NS(\vec{Q},\omega)$ and $\left(\frac{d^2\sigma}{d\Omega.dE}\right)_{inc} = b_{inc}^2 \frac{k'}{k} NS_i(\vec{Q},\omega)$

where $S(\vec{Q},\omega) = \frac{1}{2\pi\hbar}\iint G(\vec{r},t)e^{i(\vec{Q}.\vec{r}-\omega t)}d\vec{r}dt$ and $S_i(\vec{Q},\omega) = \frac{1}{2\pi\hbar}\iint G_s(\vec{r},t)e^{i(\vec{Q}.\vec{r}-\omega t)}d\vec{r}dt$

and the correlation functions that are intuitively similar to those for the elastic scattering case:

$G(\vec{r},t) = \frac{1}{N}\int\left\langle \rho_N(\vec{r},0)\rho_N(\vec{r}+\vec{R},t)\right\rangle d\vec{r}$ and $G_s(\vec{r},t) = \frac{1}{N}\sum_j\int\left\langle \delta(\vec{r}-\vec{R}_j(0))\delta(\vec{r}+\vec{R}-\vec{R}_j(t))\right\rangle d\vec{r}$

$$I(Q,\omega) = \frac{\sigma_c}{\sigma_c + \sigma_i} S(Q,w) + \frac{\sigma_i}{\sigma_c + \sigma_i} S_{self}(Q,\omega)$$

Summarise

- The intensity of ***elastic***, ***coherent*** neutron sattering is proportional to the ***spatial Fourier transform*** of the Pair correlation function, ***G(r).***
- The intensity of the ***inelastic coherent*** neutron scattering is proportional to the ***space and time Fourier transforms*** of the time dependent Pair correlation function ***G(r,t)*** - probability of finding a particle at r and t when there is another particle at r = 0 and t = 0.
- The intensity of the ***inelastic incoherent*** neutron scattering is proportional to the space and time Fourier transforms of the time dependent ***Self correlation function*** $G_S(r,t)$ - probability of finding a particle at r and t when the same particle was at r = 0 and t = 0.

Inelastic Scattering

Coherent

- X-rays – can be both spatially coherent & Incoherent – Scattering always coherent
- Neutrons – Always spatially incoherent – Coherent scattering originates for materials with structural order or spin-isotopic homogeneity

Incoherent

- X-rays – Mainly originates from Compton scattering (single component atomic system)
- Neutrons – originates from variation of isotopic composition as well as spin fluctuation (I+1/2 or I-1/2)

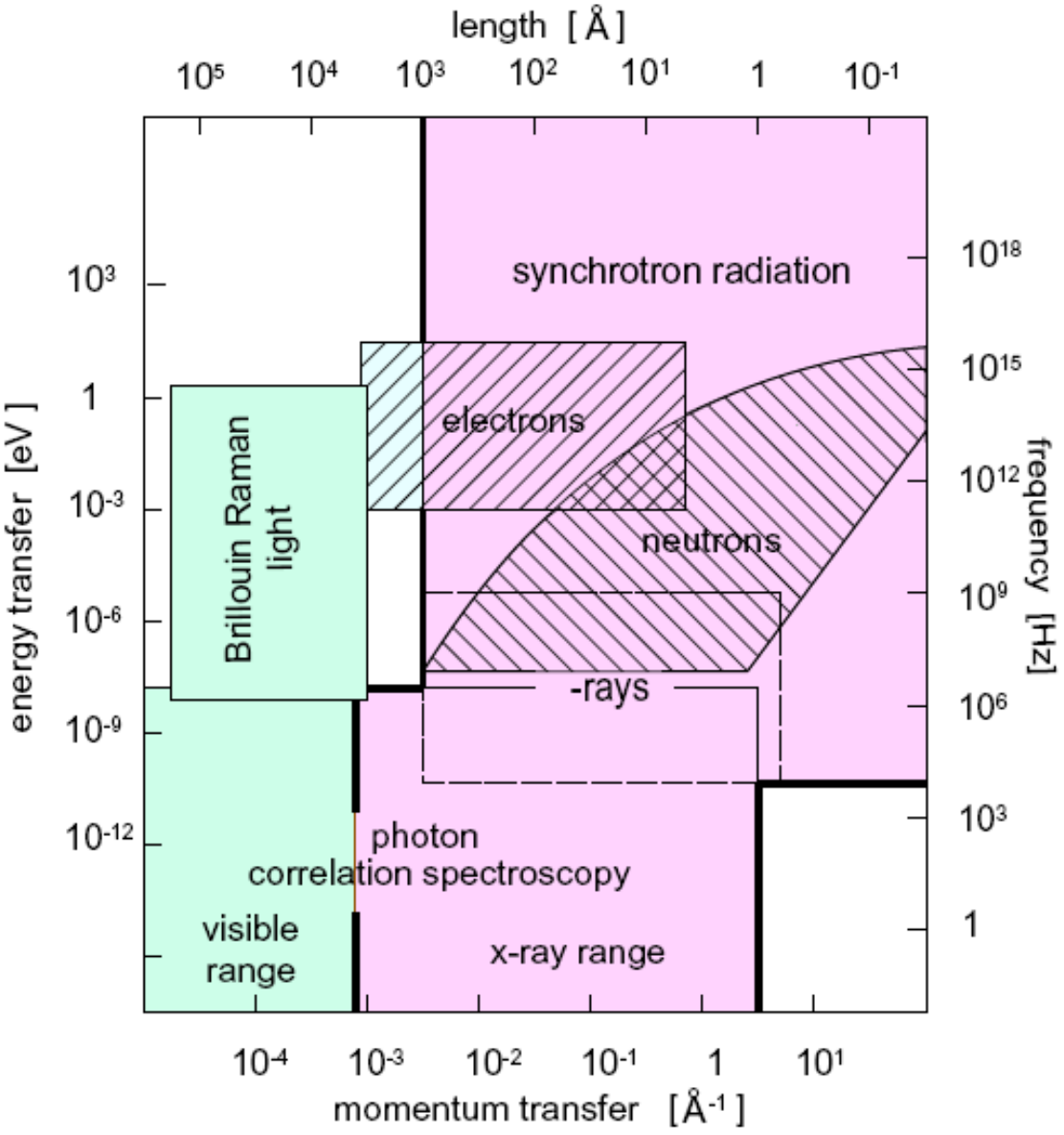

E. Burkel, Rep Prog Phys 63, 171 (2000)

Inelastic Scattering Techniques – for Glass Dynamics

- X-ray photon correlation Spectroscopy
- Inelastic/Backscattering X-ray Spectroscopy
- Inelastic Neutron Scattering
- Neutron Spin Echo Spectroscopy

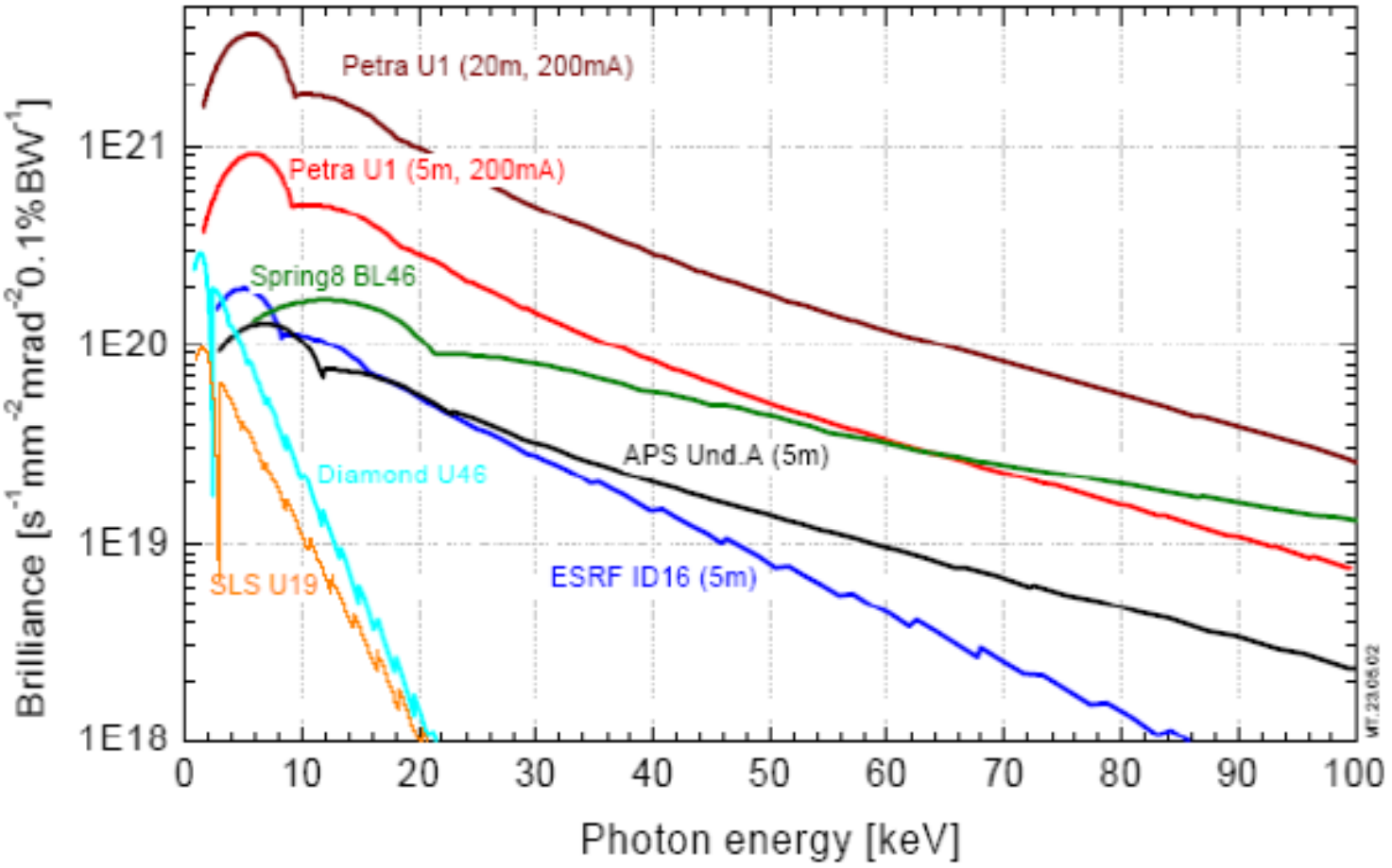
Petra U1 (20m, 200mA)
Petra U1 (5m, 200mA)
Spring8 BL46
APS Und.A (5m)
Diamond U46
ESRF ID16 (5m)
SLS U19
Brilliance [s-1mm-2mrad-20.1%BW-1]
1E21
1E20
1E19
1E18
0
10
20
30
40
50
60
70
80
90
100
Photon energy [keV]

Synchrotrons.. Fun place …

ESRF, Grenoble, France

APS, Chicago, USA

XPCS-Basics

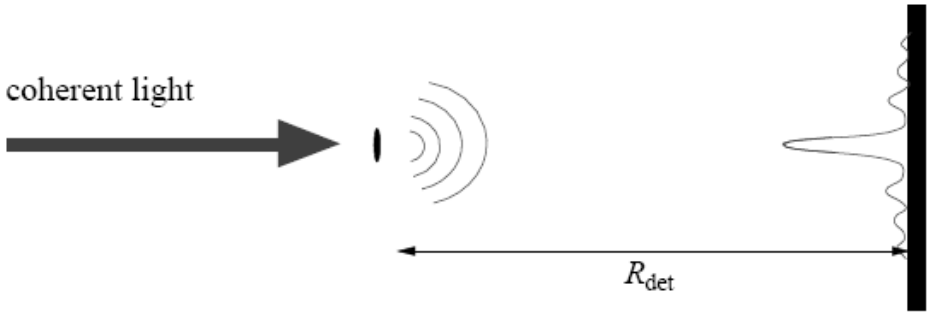

$$\xi_t = \frac{\lambda R}{w}$$

Speckle

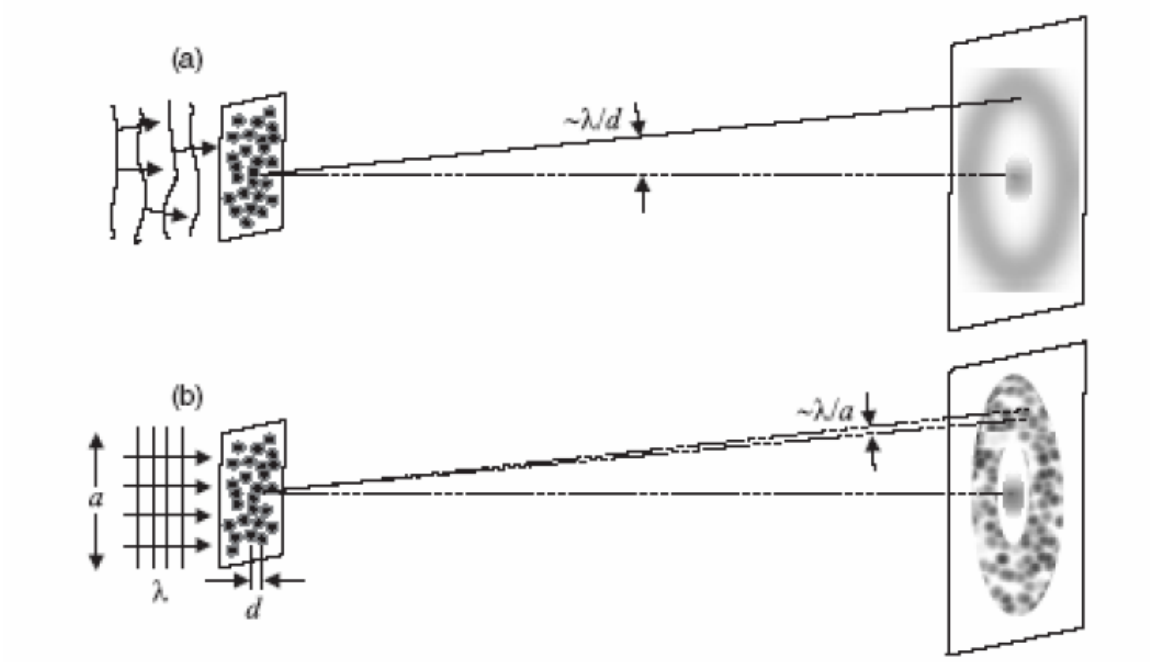

Coherence Length and Contrast

It is generally convenient to assume the source has a Gaussian intensity profile

$$I(x) = \frac{I_0}{\sqrt{2\pi}\xi} \exp\left[- \left| x - x_0 \right|^2 / 2\sigma^2 \right]$$

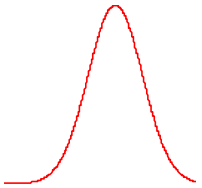

One can then define a coherence length

$$\xi = \frac{\lambda R}{2\sigma\sqrt{\pi}}$$

This characterizes the distance over which two slits would produce an interference pattern, or more generally the length scale over which any sample will produce interference effects.

A more rigorous theory can be found in e.g. Born and Wolf

Longitudinal coherence

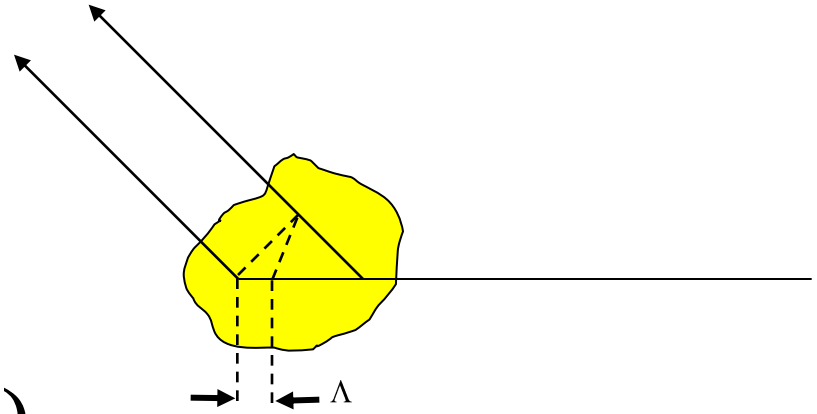

$$\Lambda \approx \lambda(E / \Delta E)$$

e.g. the number of wavelengths that can be added before the uncertainty adds up to a full wavelength.

Can also be viewed as a coherence time $T_c = \Lambda/c$

How Practical is it to Make X-rays Coherent?

Consider a point 65 meters downstream of an APS Undulator A

$$\lambda = 0.2\text{nm}, \quad \Delta\lambda/\lambda = 3\times10^{-4}$$

Ge 111

$$\sigma_x = 254\mu\text{m}, \sigma_y = 12\mu\text{m}$$

$$\xi_x = \frac{\lambda R}{2\sigma_x\sqrt{\pi}} = 14\mu\text{m}$$

$$\xi_y = \frac{\lambda R}{2\sigma y\sqrt{\pi}} = 306\mu\text{m}$$

$$\Lambda = 0.66\mu\text{m}$$

$\sim 3\times10^{10}$ Photons/Coherence Area

XPCS-Basics

Observation of speckles depends on the spatial and temporal coherence of the source. The degree of spatial coherence of a slit-shaped source is defined as

$$|\mu(\Delta x)| = \left|\frac{\sin(\nu)}{\nu}\right| , \quad \nu = \Delta x \frac{ak}{2R_{\text{source}}} ,$$

a is the slit width.

The spatial autocorrelation of speckles

$$C_{\vec{r}}(\Delta\vec{r}) \equiv \frac{\left\langle I(\vec{r})\ I(\vec{r}+\Delta\vec{r})\right\rangle_{\vec{r}}}{\left\langle I(\vec{r})\right\rangle_{\vec{r}}\left\langle I(\vec{r}+\Delta\vec{r})\right\rangle_{\vec{r}}} - 1$$

The speckle contrast Γ

$$\Gamma(\vec{r}) \equiv C_{\vec{r}}(0) = \frac{\sigma^2_{I,\vec{r}}}{\left[\left\langle I(\vec{r})\right\rangle_{\vec{r}}\right]^2}$$

$$g_2(\tau,\vec{q}) \equiv \frac{\left\langle I(t,\vec{q})\, I(t+\tau,\vec{q})\right\rangle_t}{\left[\left\langle I(t,\vec{q})\right\rangle_t\right]^2} - 1$$

Speckle Patterns

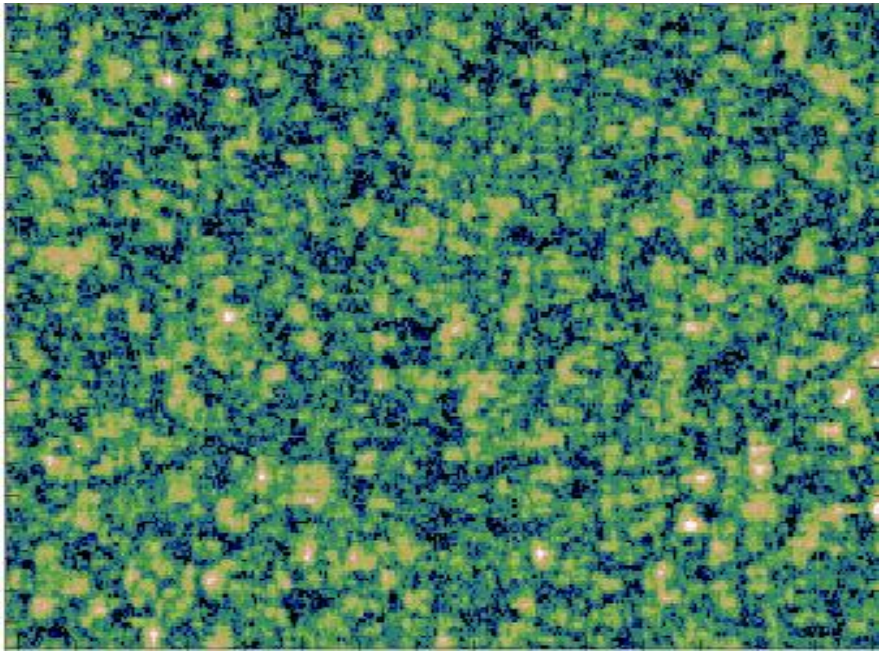

Silica Aerogel

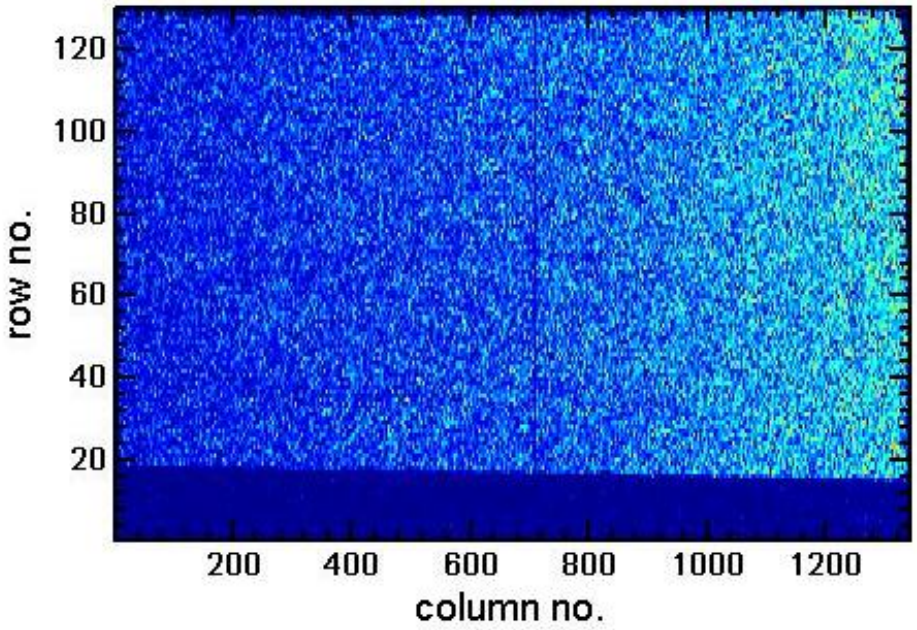

Nanoparticles in Polymers

Examples of some typical time correlations

Physical Process	Theoretical Form of $g_2(\tau, q)$
Translational diffusion of single species	$A + B \exp\left(-2Dq^2\tau\right)$
Translational diffusion in polydisperse samples	$A + \left[\int B(M) \exp\left(-D(M)q^2\tau\right) \mathrm{d}M\right]^2$
Rotational diffusion of single species	$A + \left[\sum_{l=\text{even}} B_l \exp\left(-\left[Dq^2 + l[l+1]/\tau_R\right]\tau\right)\right]^2$
Flexing molecules	$A + \left[\sum_{m,n} P_{m,n} \exp\left(-[Dq^2 + m/\tau_n]\tau\right)\right]^2$
Motile objects	$A + B \exp\left(-\tau^2/2\tau_d^2\right)$
Directed motion; propagating waves on a surface	$A + B \exp(-\tau/\tau_d)\cos(\omega\tau)$

Experimental Aspects

Optical elements	Double mirror	Mono I	Mono III
Distance from source	36 m	44.2 m	56.8 m
Focusing	Be CRL @ 24 m from the source for vertical focusing at Troika I and Troika III at 8keV. Vertical focusing with double mirror.		
Beam size at sample	Max: 2×0.8 mm^2 (h × v) ; Coherent: 10×10 μm^2		
Energy range	7-20keV; Coherent: 7-13 keV (Troika I), 7-20 keV (Troika III)		
Energy resolution ΔE/E	Mono I (single bounce): 5.9×10^{-5} C(111), 2.3×10^{-5} C(220), 1.4×10^{-4} Si(111) Mono III (channel cut): 1.4×10^{-4} Si(111)		
Flux at sample	~ 5×10^{13} ph/s/mm^2. Coherent intensity >10^9 ph/s (8 keV, 10×10 μm^2 beam size) Brilliance >10^{20} ph/s/mm^2/mrad^2/0.1%bw/100mA @ 8keV		

Setup for XPCS at Sector 8 of the APS

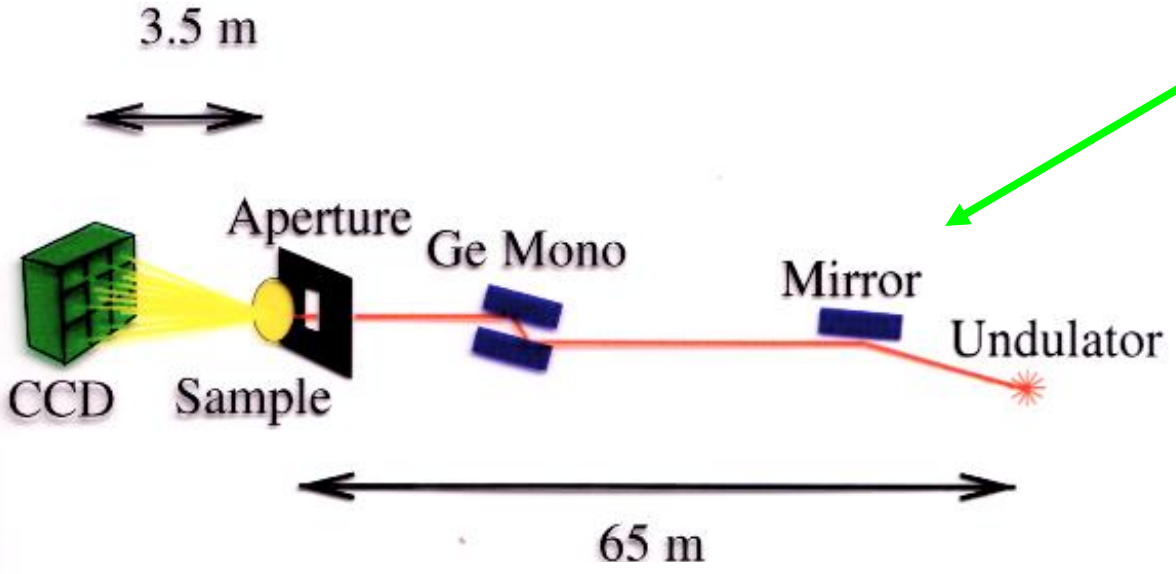

Transmission

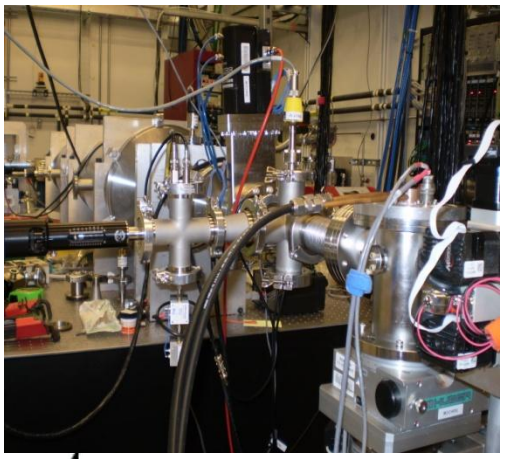

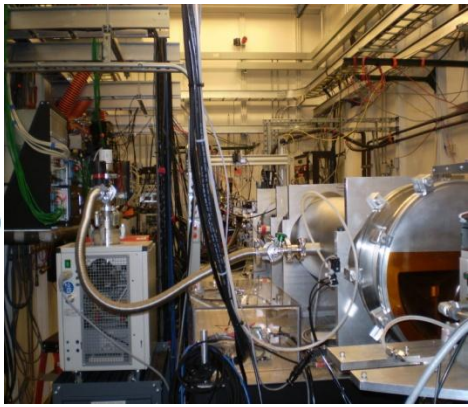

CCD

Reflection

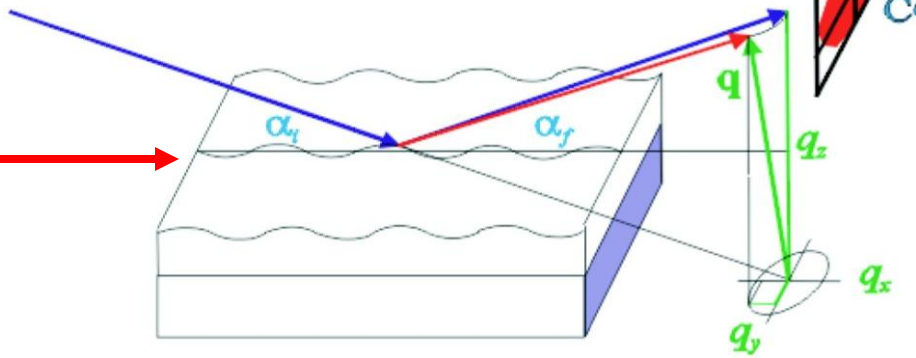

Applications of XPCS

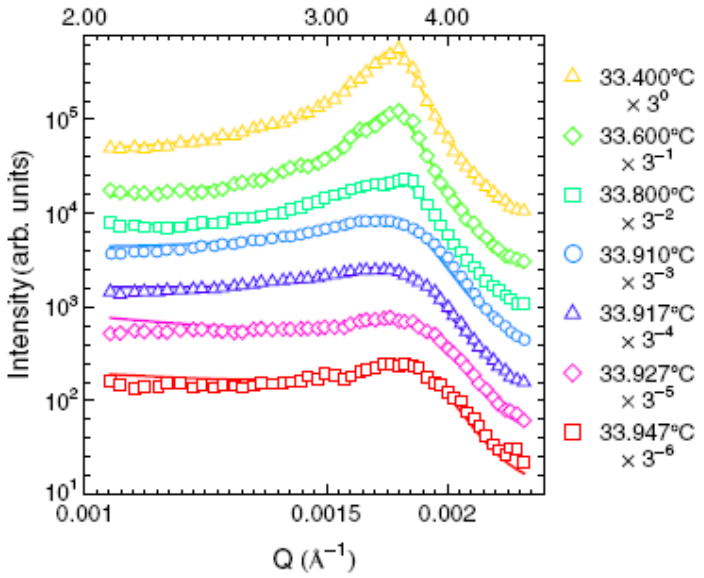

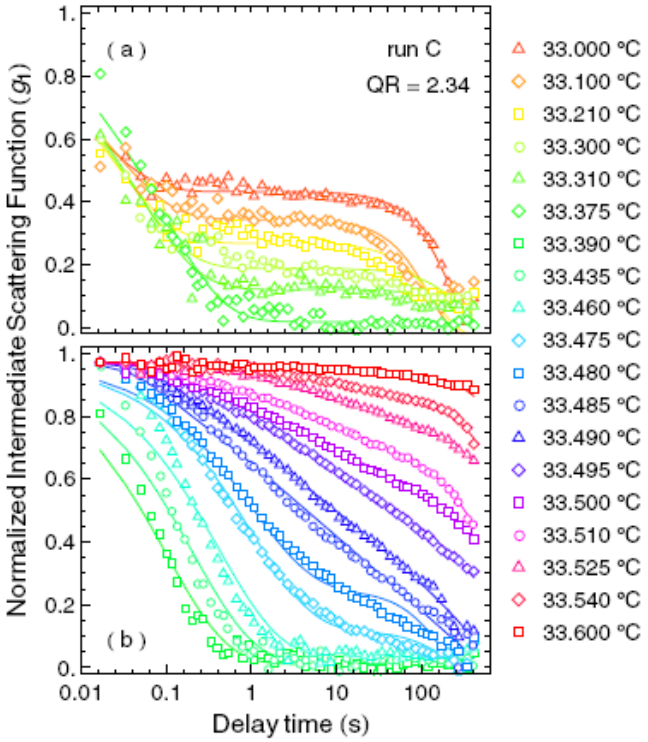

Silica nanoparticles in Water-Lutidine near critical binary mixture

How a liquid becomes glass on cooling and heating

Lu et al, PRL 100, 045701 (2008)

Applications of XPCS

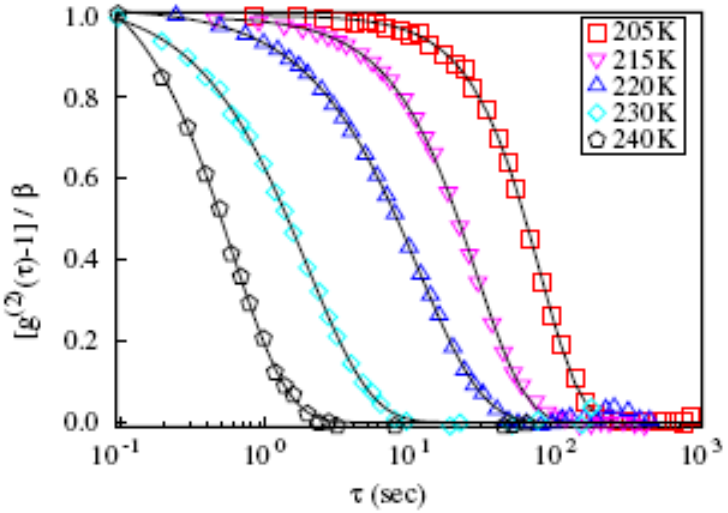

$$g^{(2)}(\tau) = \beta \exp[-2(\Gamma\tau)^{\gamma}] + 1,$$

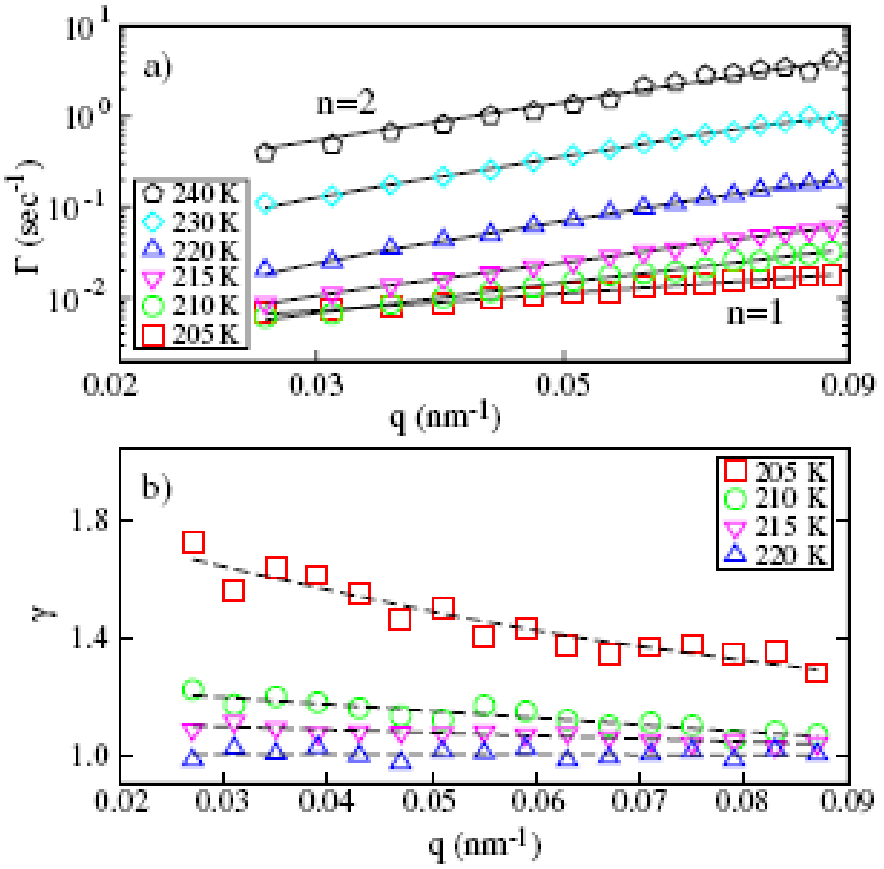

Dynamics of Nanoparticles in supercooled liquids (Propanediol) T_G = 170K

Caronna et al, PRL 100 055702 (2008)

Applications of XPCS

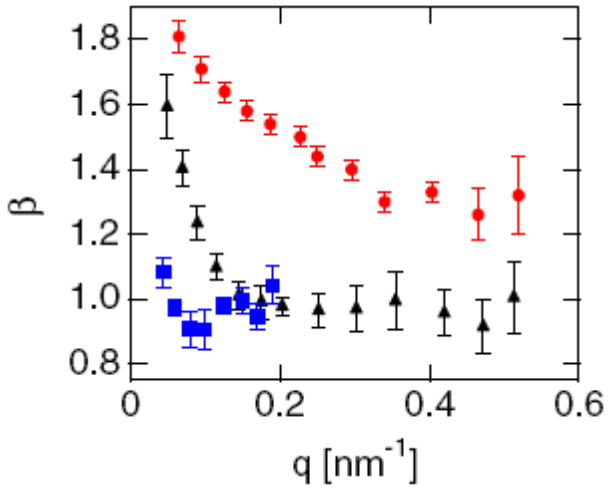

FIG. 2 (color online). Stretching exponent vs wave vector for Au nanoparticles in a PS melt, $M_W = 2000$ g/mol, at 303 K (circles), 313 K (triangles), and 323 K (squares).

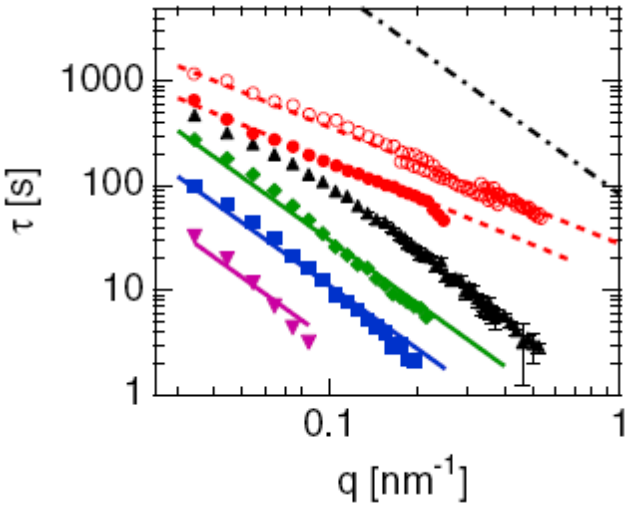

FIG. 3 (color online). Correlation time vs wave vector for $M_W = 2000$ g/mol at 303 K (circles), 313 K (triangles), 318 K (diamonds), 323 K (squares), and 333 K (inverted triangles). The results at 303 K were obtained 46 min (solid circles) and 166 min (open circles) after cooling from 313 K. The solid lines are from fits to $\tau = 1/Dq^2$; the dashed lines are from fits to $\tau = A/q$. The dash-dotted line gives the correlation times at 303 K expected for diffusion extrapolated from high temperatures.

T_G = 275K

Nanoparticle motion within glassy polymer melts

Guo et al, PRL 102, 075702 (2009)

Applications of XPCS

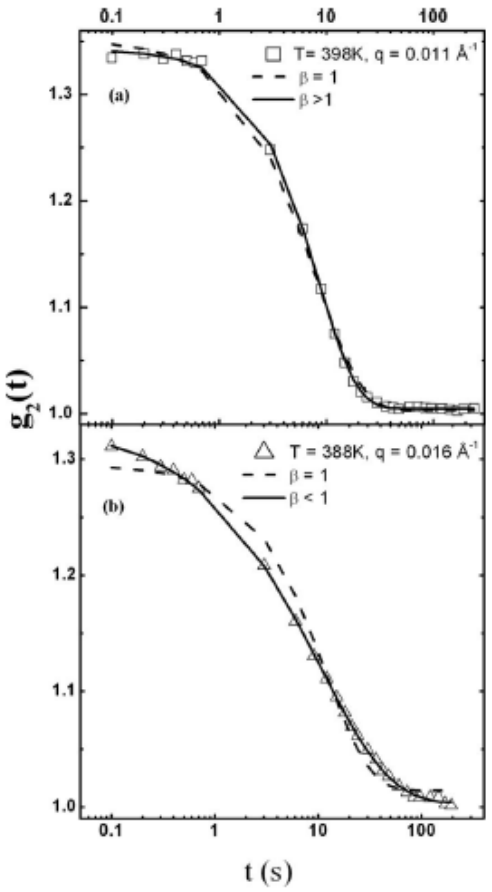

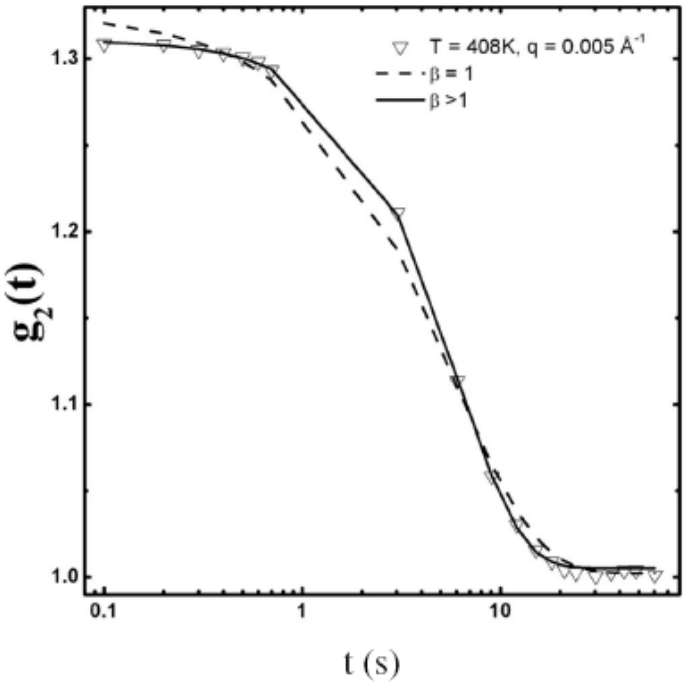

$$G_1(Q,t) = A\exp-\left(\frac{t}{\tau}\right)^{\beta}$$

Complex dynamics in polymer nanocomposites

S Srivastava et al PHYSICAL REVIEW E **79**, 021408 (2009)

Applications of XPCS

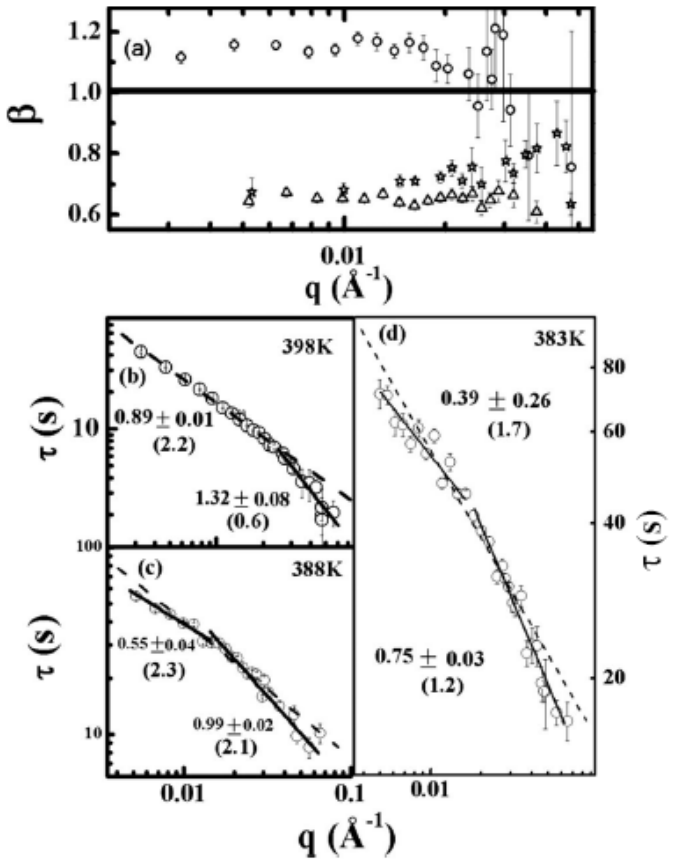

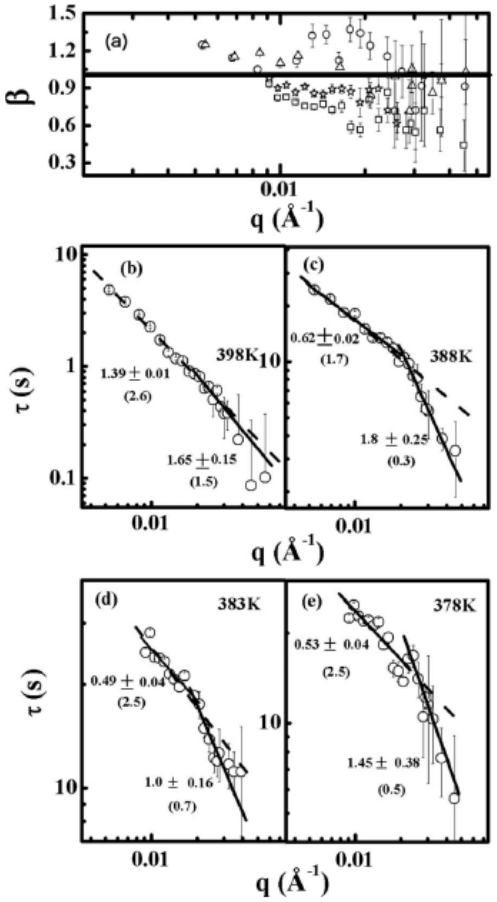

$$G_1(Q,t) = A\exp-\left(\frac{t}{\tau}\right)^{\beta}$$

Complex dynamics in polymer nanocomposites

S Srivastava et al PHYSICAL REVIEW E **79**, 021408 (2009)

Applications of XPCS

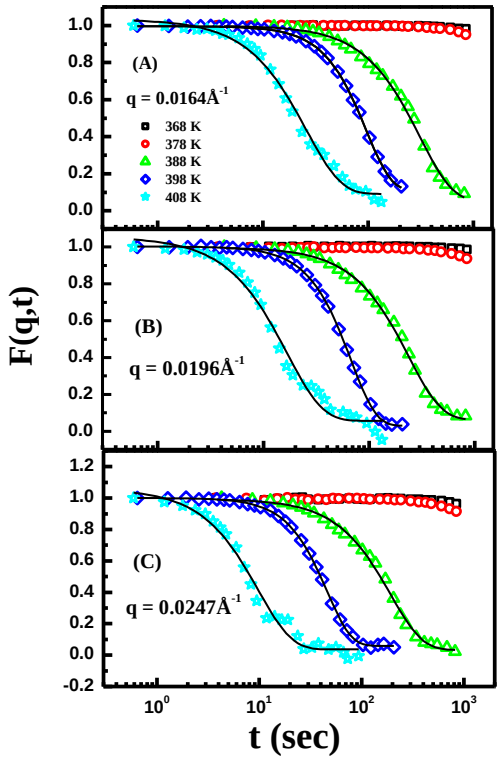

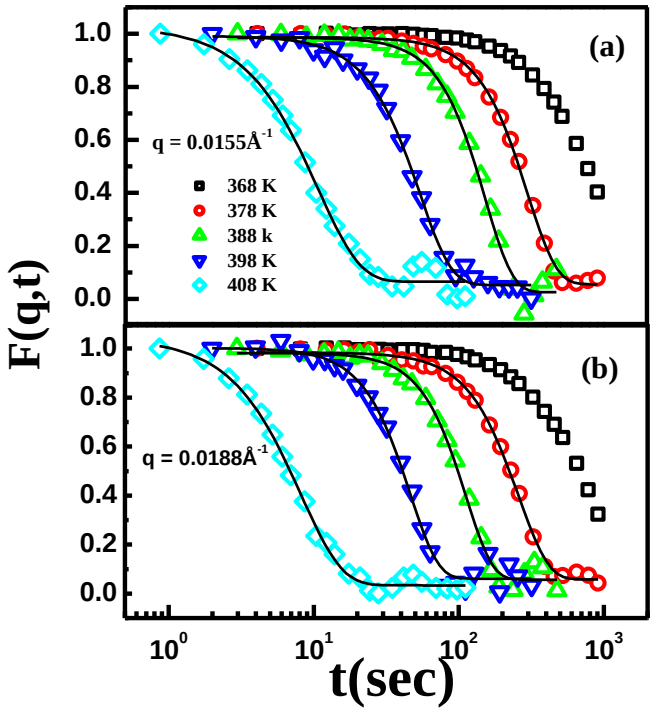

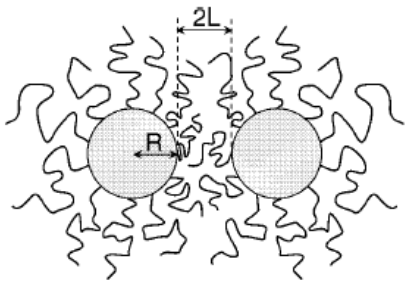

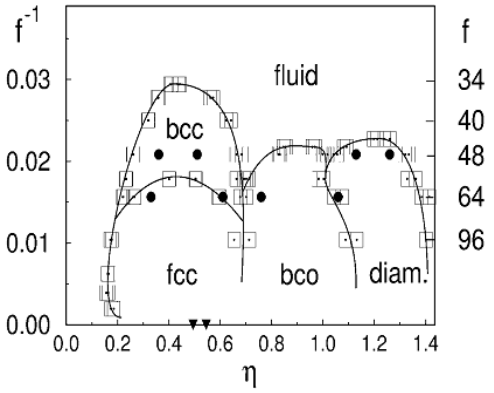

Low Grafting Density

High Grafting Density

Unusual dynamical arrest in polymer grafted nanoparticles

A Kandar et al

THE JOURNAL OF CHEMICAL PHYSICS **130**, 121102 (2009)

Inelastic X-Ray Scattering (IXS)

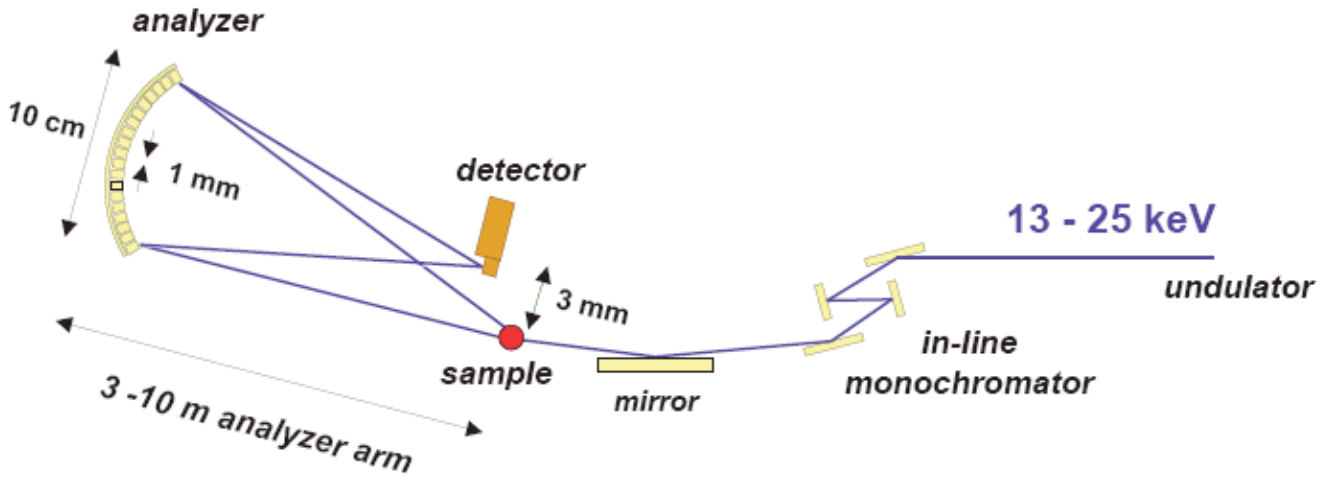

Energy resolution: 10 - 1 meV

$\delta E \sim 1/E^4$!

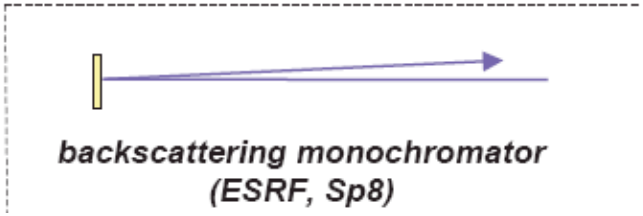

IXS - Examples

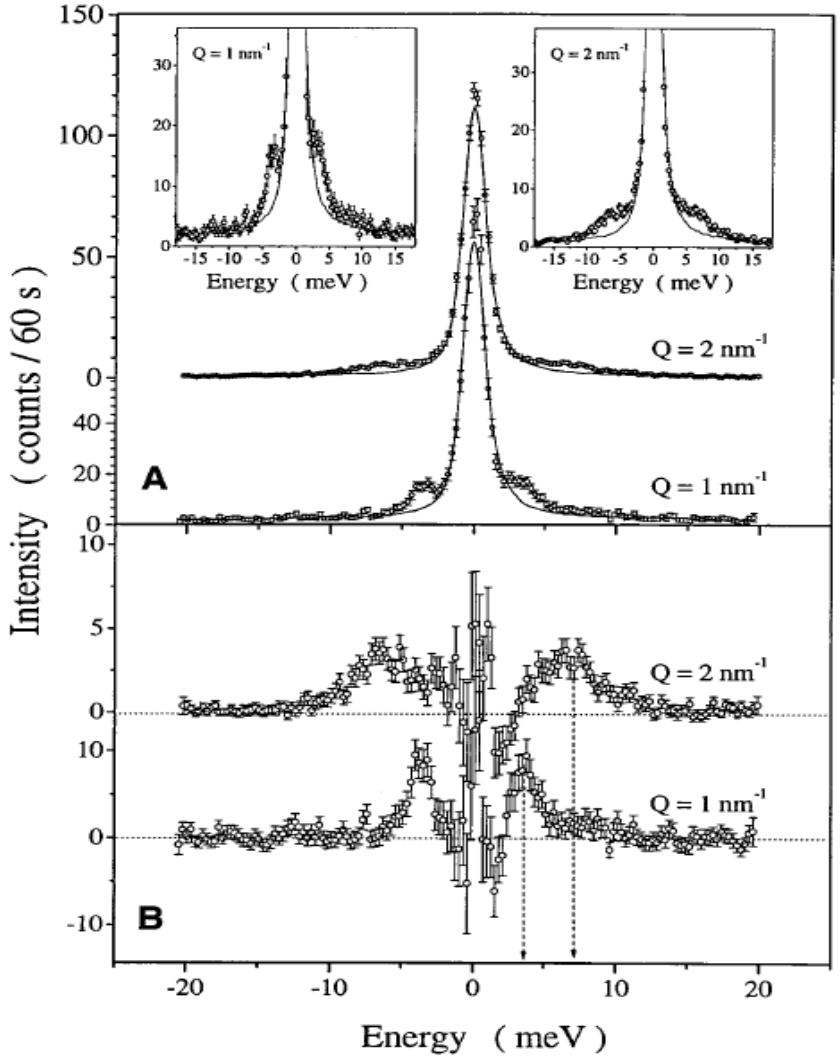

Boson Peak in Silica

Sette, Science 280, 1550 (1998)

Fig. 1. (**A**) IXS spectra (○) of vitreous silica taken at T = 1075 K at Q = 1 and 2 nm^{-1}, with a total integration time of 415 and 800 s, respectively. The full curves are the measured resolution functions, which have been aligned and scaled to the central peak. The two insets are shown to emphasize the inelastic signal on the two sides of the central peak. (**B**) Difference spectra, obtained from the subtraction of the scaled resolution function from the spectra reported in (A). The inelastic peak energy positions, indicated by the dotted lines with arrows, scale approximately with the Q transfer.

IXS - Examples

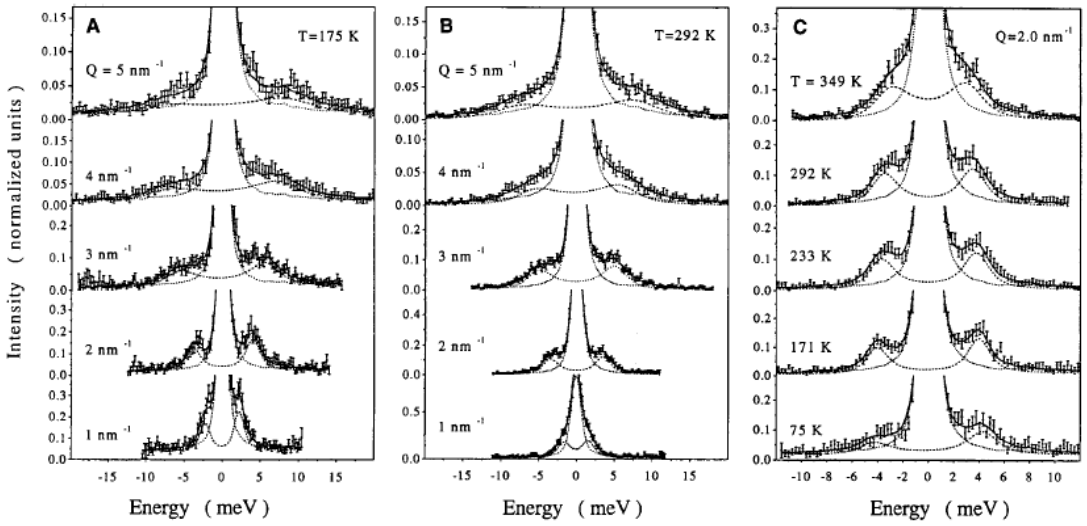

IXS spectra of Glycerol

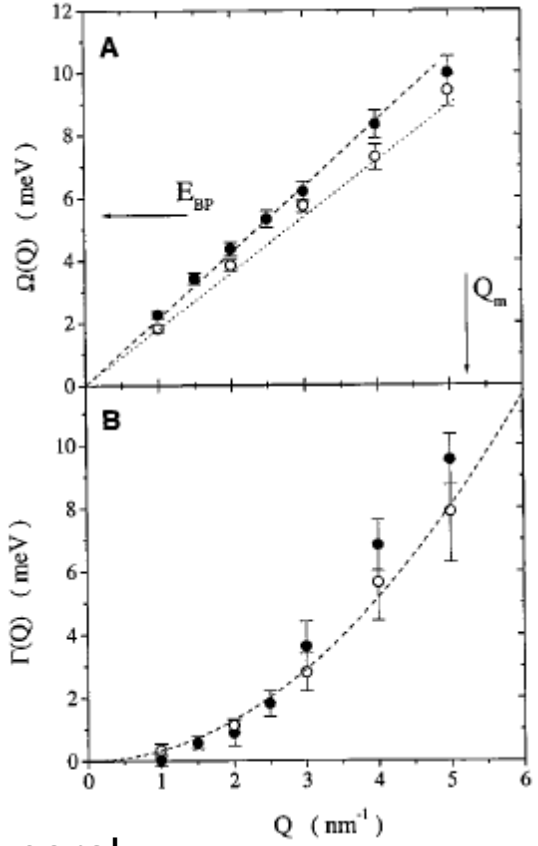

Boson Peak in Glycerol

Sette, Science 280, 1550 (1998)

IXS - Examples

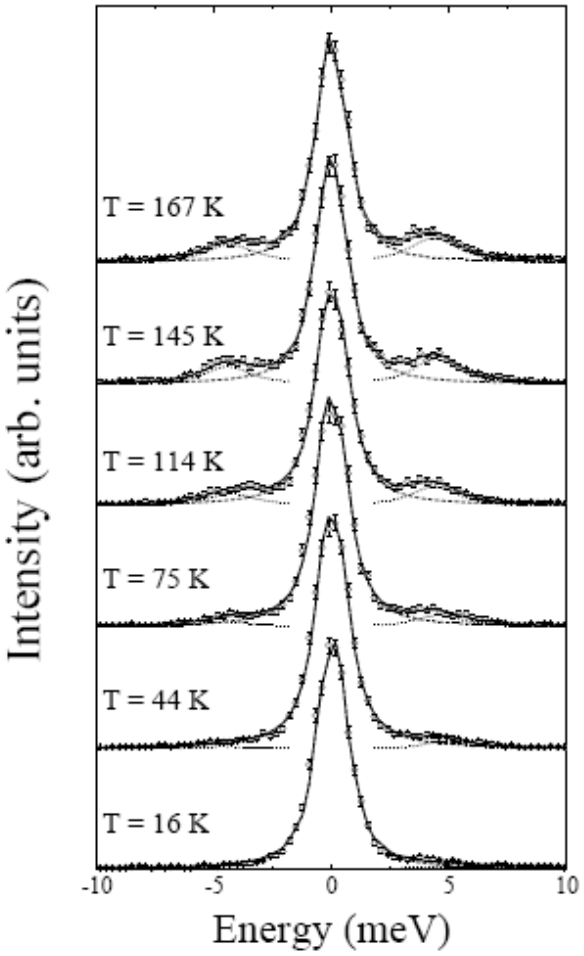

IXS spectra of Glycerol

Sample	$T_g[K]$	m	α
BeF_2[a]	598	20	0.16
silica[b]	1450	28	0.19
glycerol[c]	190	53	0.32
$PB_{1.4}$[d]	180	60	0.40
nBB[e]	125	53	0.46
salol[f]	218	73	0.64
mtol[g]	187	77	0.57
oTP[h]	241	81	0.58
mTCP[i]	205	87	0.59
Se[j]	308	87	0.7

$$m = \lim_{T \to T_g} \frac{d\log(\eta)}{d(T_g/T)}$$

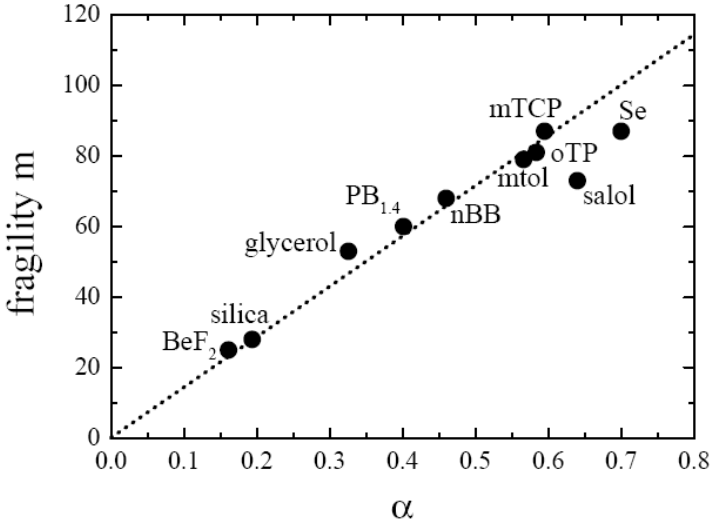

The parameter α is a property of the glass phase as extracted from the IXS measurement.

Scopigno, Sette, Science (2003)

Neutron Scattering - Sources

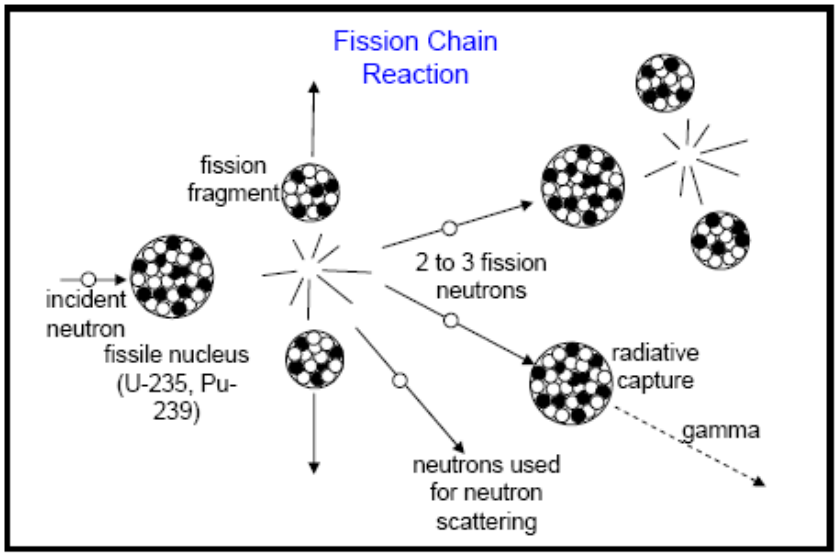

NEUTRON SOURCES

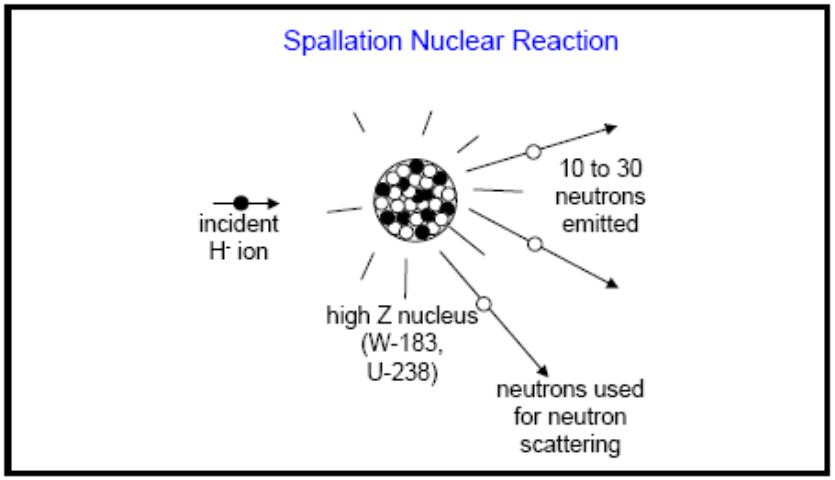

Willis & Carlile, Experimental Neutron Scattering, OUP (2009)

Neutron Scattering - Sources

CONTINUOUS VS TIME-OF-FLIGHT

Continuous
Reactors

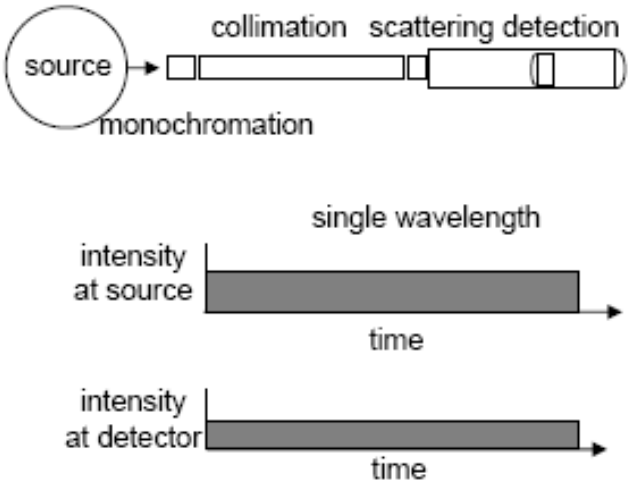

Measure some of the neutrons all of the time

Pulsed Sources

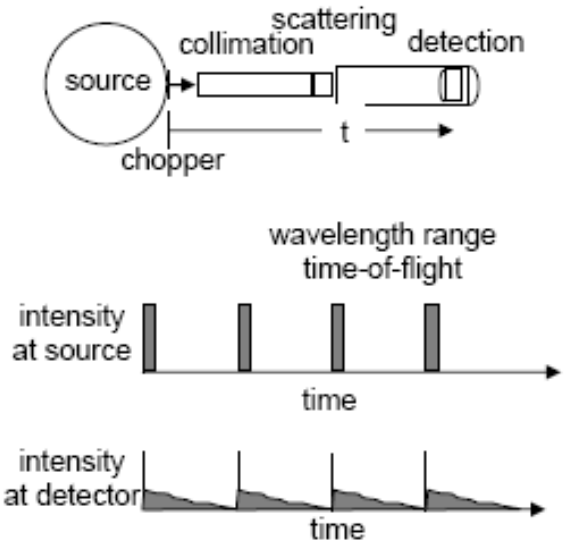

Measure all of the neutrons some of the time

Neutron Scattering - Sources

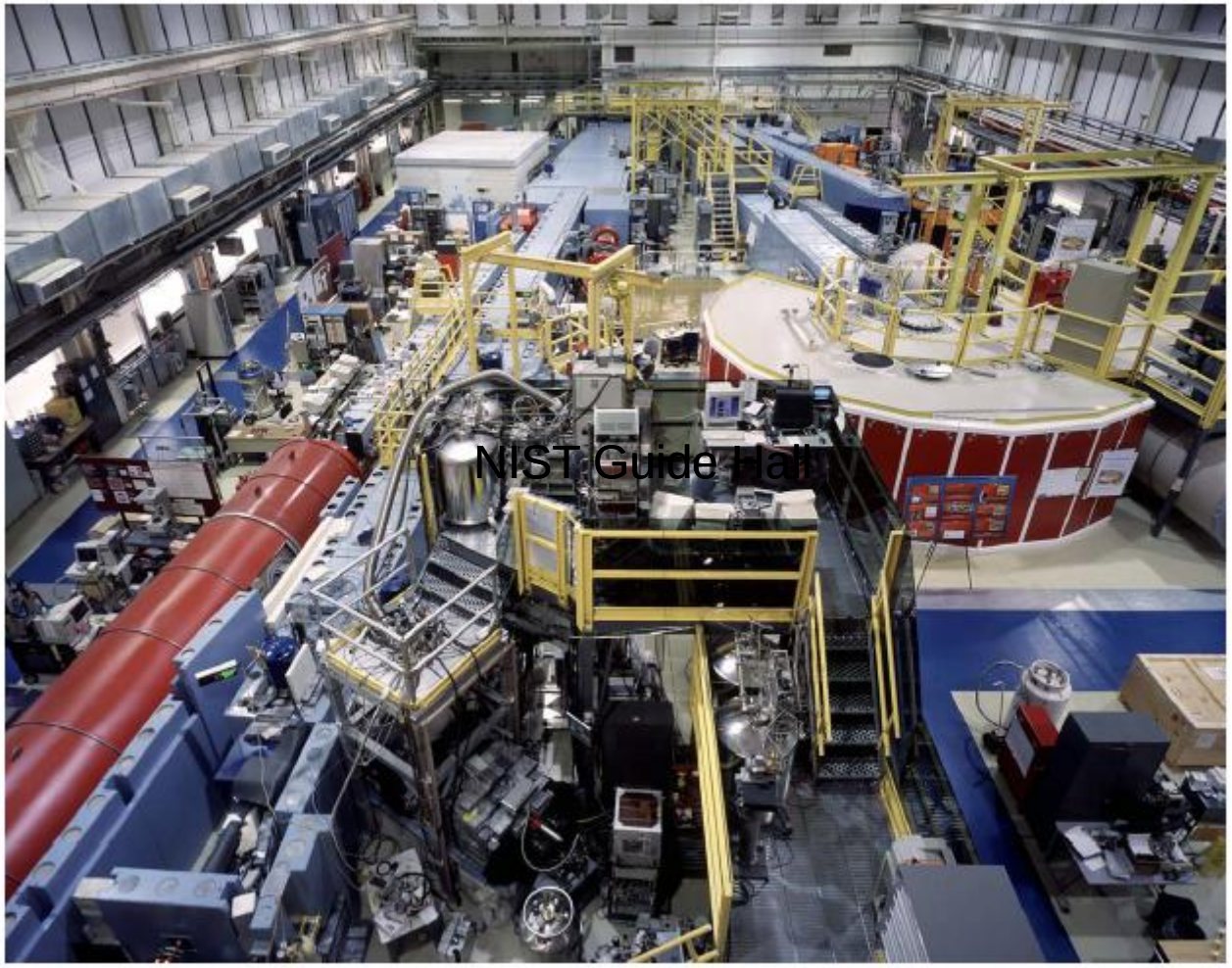

Reactor

Neutron Scattering - Sources

Spallation Neutron Source, Oak Ridge

Spallation

Neutron Scattering - Sources

High Resolution Backscattering Spectrometer @ SNS

Inelastic Neutron Scattering

- Reactors – Triple Axis Spectrometer – Scan to get Energy and Momentum Transfer
- Spallation sources – Time-of-Flight spectrometers – Either Fixed incident energy (Direct) or Fixed Scattered (Indirect)

Neutron Spin Echo Spectroscopy

$$\frac{dL}{dt} = \frac{g_n \mu_n}{h}(L \times B)$$

L is the neutron spin angular momentum, g_n is the Lande g factor and B is the external mag field.

The Larmor frequency, ω_L

$$\omega_L = \frac{g_n \mu_n}{h} B$$

Neutron Spin Echo Theory

Precession angle mismatch:

sensitivity proportional to λ^3

$$\Delta\phi = \left(\frac{2\pi |g_n| \mu_N m_n}{h^2}\right) Bl\,(\lambda_f - \lambda_i) \approx \underbrace{\frac{|g_n| \mu_N m_n \lambda^3 Bl}{h^3}}_{t_{NSE}(B)} \omega$$

time parameter proportional to B and current

$\Rightarrow$ Loss of polarization:

$$P = \cos\Delta\phi$$

... averaged over all scattered neutrons:

$$P(Q, t_{NSE}) = \frac{\int_{-\infty}^{\infty} S(Q,\omega)\cos(\omega t_{NSE})\,d\omega}{\int_{-\infty}^{\infty} S(Q,\omega)\,d\omega} = \frac{I(Q,t_{NSE})}{I(Q,0)}$$

Neutron Spin Echo measures directly the normalized intermediate scattering function!

F Mezei et al, Neutron Spin Echo Spectroscopy, Springer (2003)

Neutron Spin Echo Spectroscopy

Practical Neutron Spin Echo

- To start and stop the precession of the neutrons at a well defined plain, π/2 flippers are used
- For the precession in the opposite sense, instead of applying opposite B field the precession plane is turned around (π flipper)

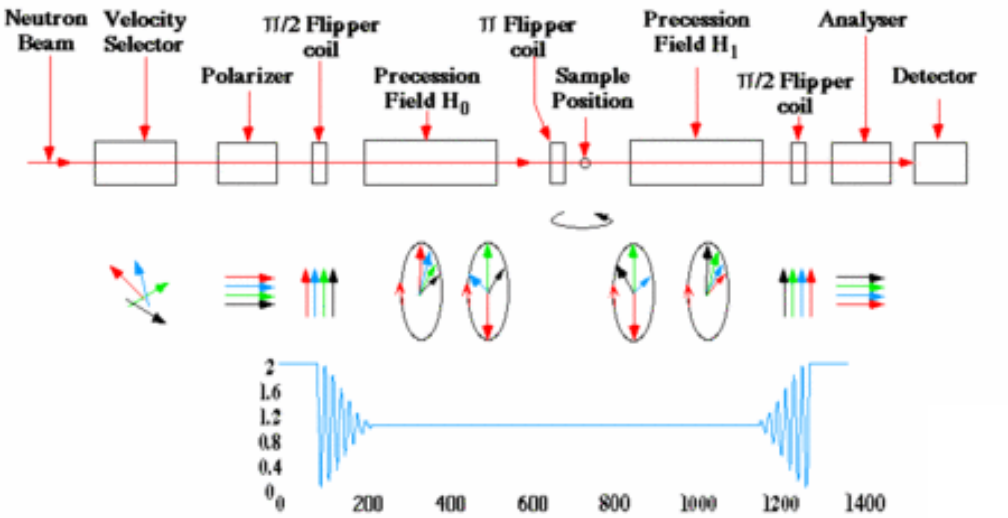

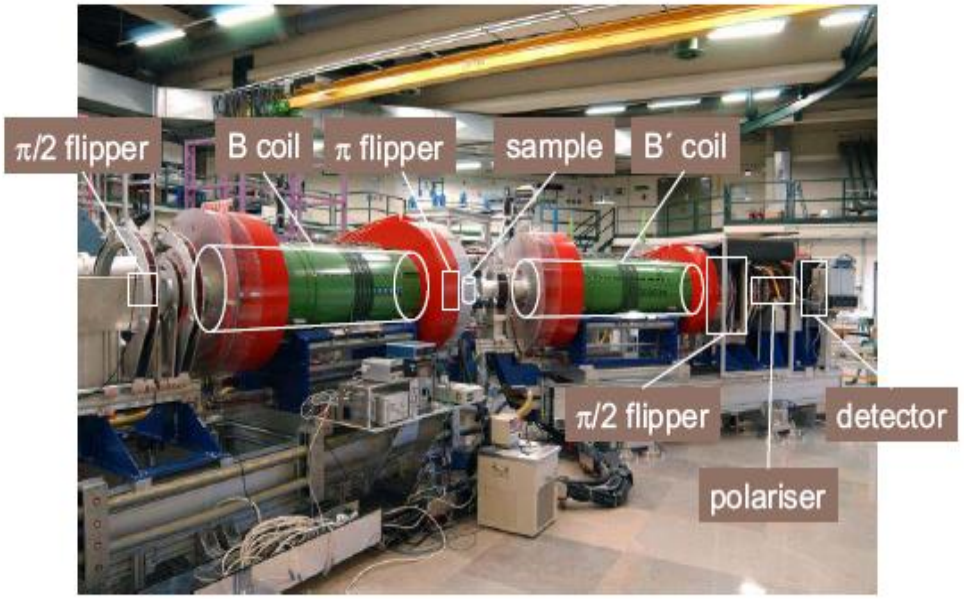

Inelastic and Quasi-elastic Neutron Scattering

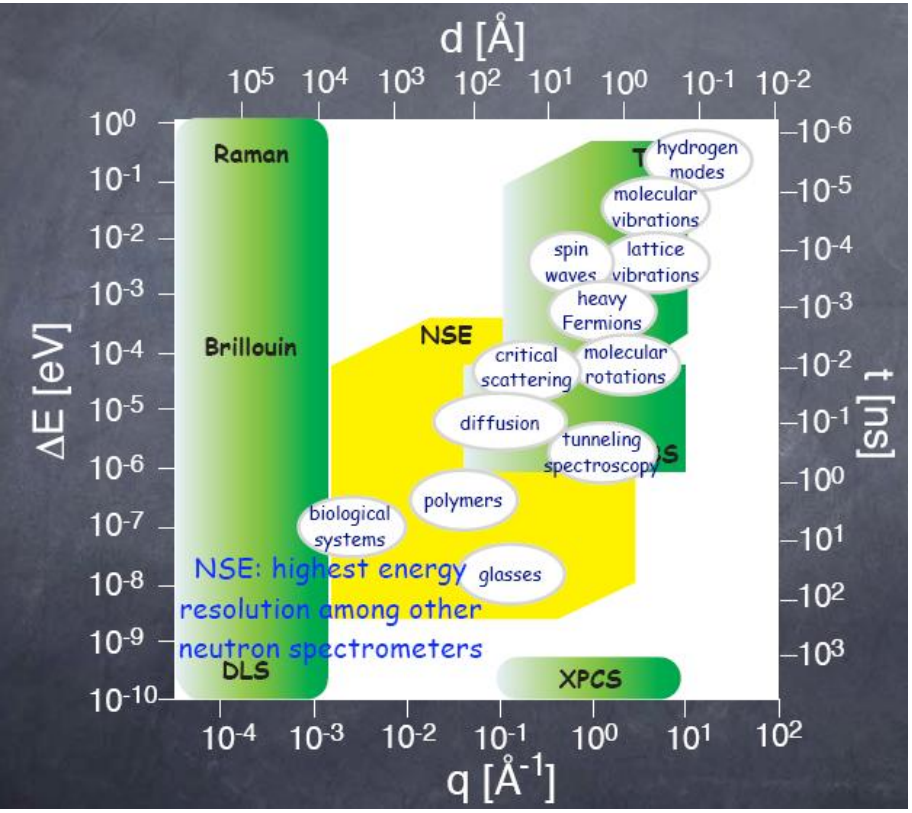

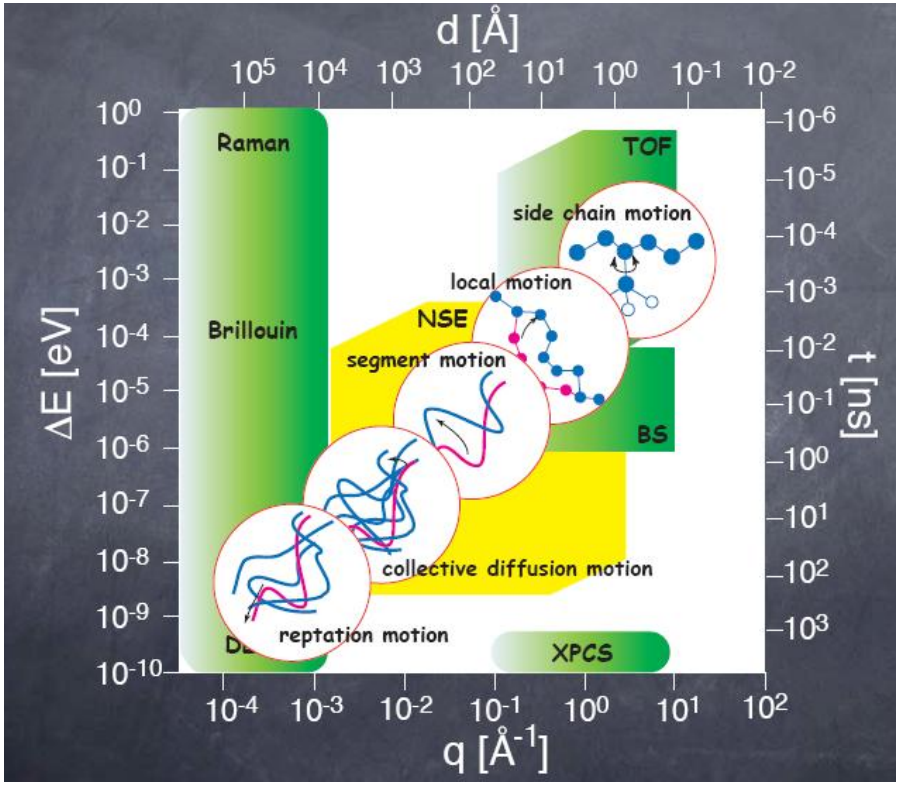

NSE - Examples

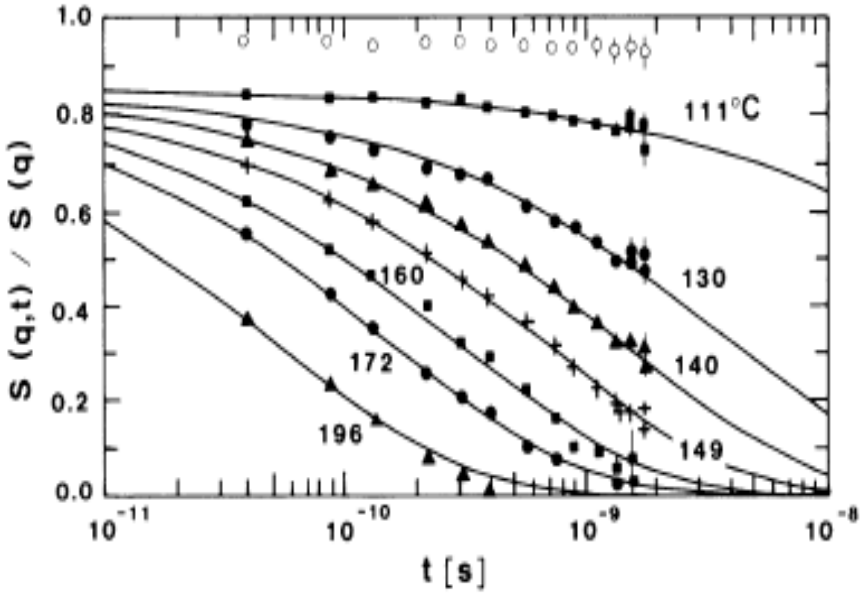

FIG. 1. The time-dependent dynamic structure factor of the $Ca_{0.4}K_{0.6}(NO_3)_{1.4}$ ionic glass system at various temperatures, as directly observed by NSE spectroscopy ($q \simeq 1.7$ Å^{-1}). The open circles are room-temperature data; for the other spectra the temperature is indicated in degrees celsius. The solid lines represent Eqs. (1) and (2) evaluated for the given temperatures with parameters obtained by fitting of the scaled plot in Fig. 2, as described in the text.

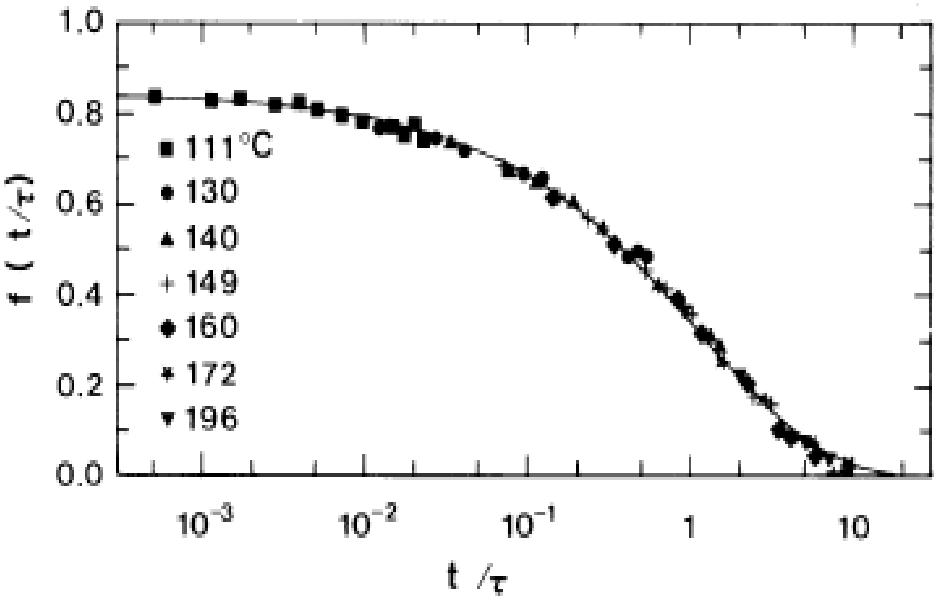

FIG. 2. The same data as in Fig. 1 plotted against the scaled time variable t/τ, where τ was calculated from Eq. (2). The solid line represents Eq. (1) with the best choice of parameters A, β, and the position of the $t/\tau = 1$ point on the abscissa. Overlapping data points have only been plotted for one of the temperatures.

Neutron Spin-Echo study of Dynamic Correlations near the Liquid-Glass Transition

Mezei et al , PRL 58 571 (1987)

NSE - Examples

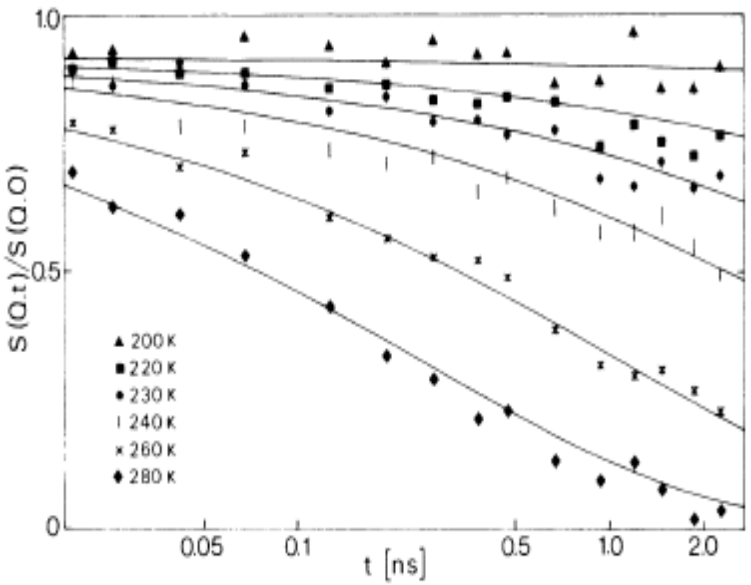

FIG. 2. Neutron-spin-echo spectra obtained near the maximum of $S(Q)$ ($Q = 1.48$ Å^{-1}) for various temperatures. The solid lines are the result of a combined fit to a Kohlrausch law.

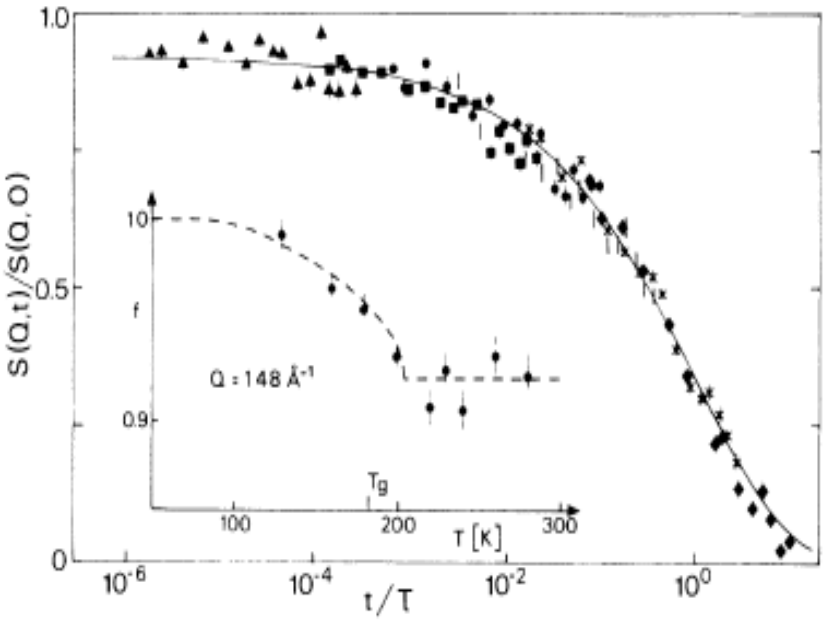

FIG. 3. Scaling representation of the spin-echo data for $Q = 1.48$ Å^{-1} (▲, 200 K; ■, 220 K; ●, 230 K, |, 240 K; ×, 260 K; ♦, 280 K). The scale $\tau(T)$ is taken from a macroscopic viscosity measurement (Ref. 7). Inset: Temperature dependence of the nonergodicity parameter $f(Q)$ near the maximum of $S(Q)$ ($Q = 1.48$ Å^{-1}).

Neutron Spin-Echo investigation on the dynamics of polybutadiene near the glass transition

Richter et al, PRL 61, 2465 (1988)

INS - Examples

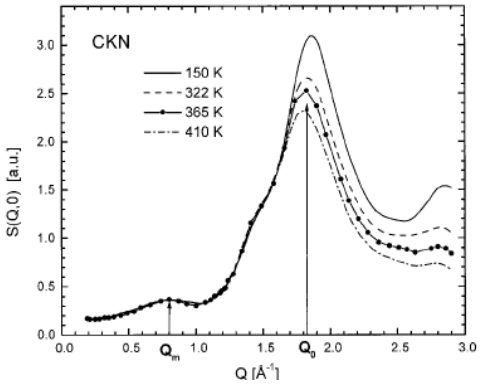

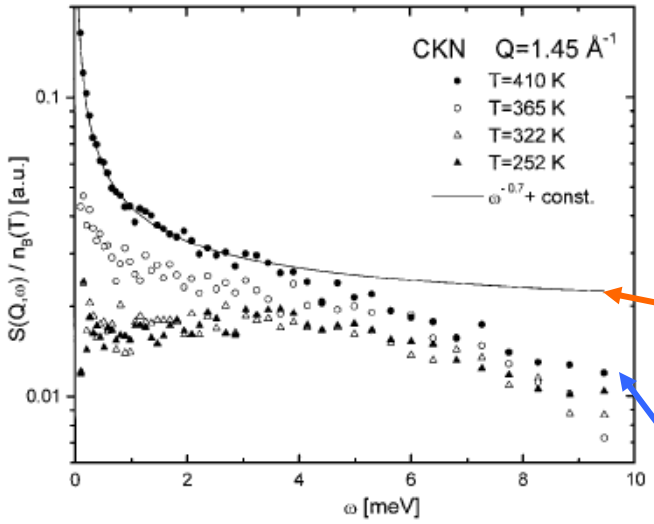

FIG. 3. Temperature dependence of the dynamic structure factor in CKN at a given Q value. The dramatic anharmonic increase of the spectral intensity above T_g corresponds to the appearance of the so-called picosecond process.

$$S(Q,\omega) = A(\omega)Q^2S(Q) + B(\omega)Q^2$$

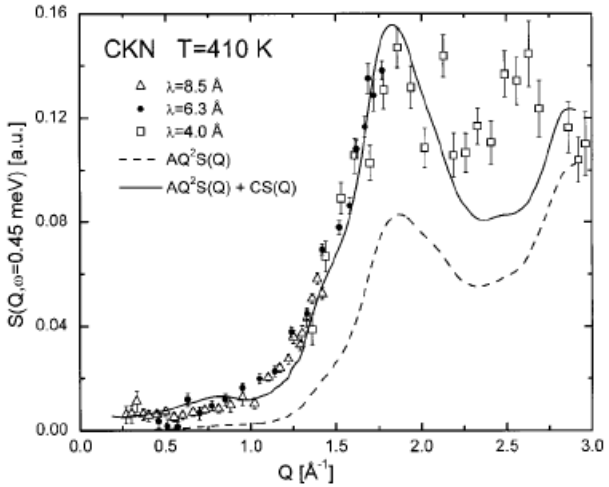

IG. 4. Wave number dependence of the dynamic structure factor at constant energy in CKN in the supercooled liquid phase. For comparison, the dashed line represents the extrapolation to this temperature of the vibrational model Eq. (1) found to well describe (actually with $B = 0$) the dynamic structure factor in the glass phase at 322 K. The continuous line was obtained by adding an additional term $CS(Q)$, as introduced in Eq. (2) with $h(Q) = 1$. Although many approximate fits are possible using Eq. (2) with different A and B combinations, at the low-Q end of the spectra these terms in Q^2 remain always much too small compared to the data points.

$$S(Q,\omega) = A(\omega)Q^2S(Q) + B(\omega)Q^2 + C(\omega)h(Q)S(Q)$$

Experimental Evidence for Fast Heterogeneous Collective Structural Relaxation in a Supercooled Liquid near the Glass Transition

Russina, Mezei et al PRL 84, 3630 (2000)

INS-Examples

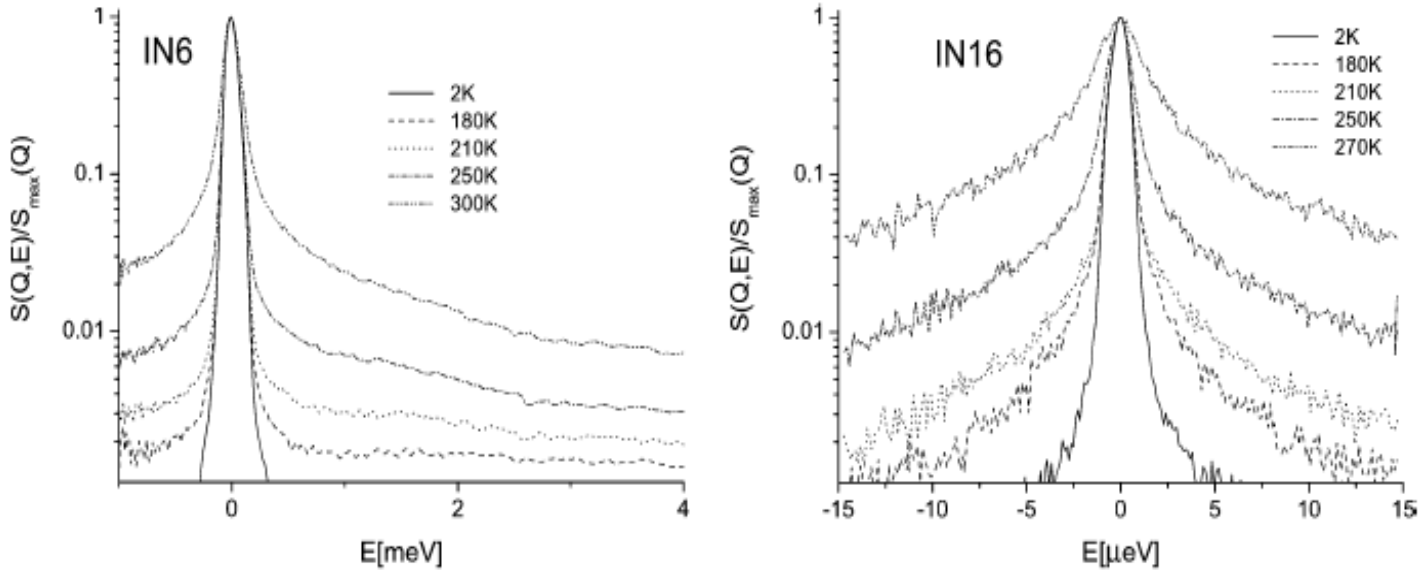

Fig. 1 Scattering function convoluted with the instrumental resolution, $\tilde{S}(Q = 1.88\ \text{Å}^{-1}, \hbar\omega)$, as obtained from instrument-specific software for neutron time-of-flight (left) and backscattering (right) spectrometers IN6 and IN16. Temperatures are indicated in the plots. The spectra at 2 K represent the resolution function. Only the standard corrections (self-shielding, empty cell background) have been done. For TOF data, in addition, spectra were interpolated to constant $Q = 1.88\ \text{Å}^{-1}$.

Inelastic neutron scattering study of a glass-forming liquid in soft confinement†

Zorn et al, Soft Matter 2008

INS-Examples

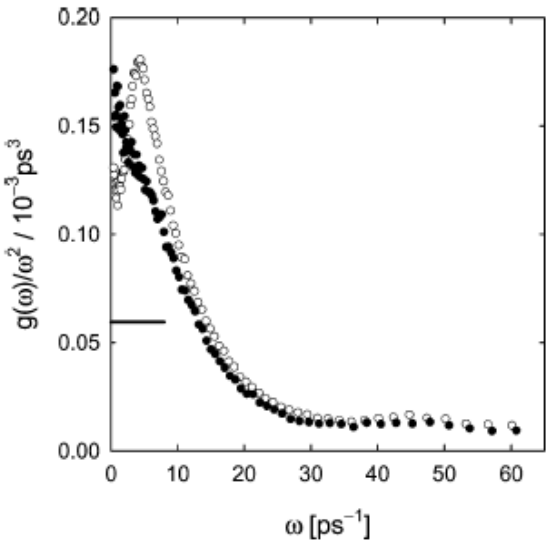

Fig. 3 Vibrational density of states (VDOS). Filled circles: PG in soft confinement; empty circles: bulk PG. Temperature used for VDOS determination: 100 K. The solid line indicates the level expected from sound waves in the Debye model.

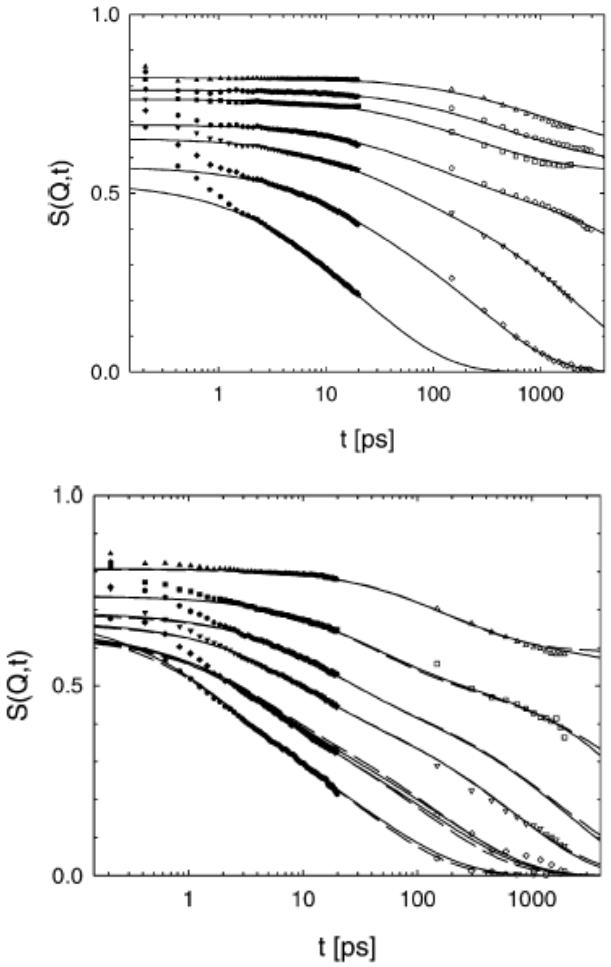

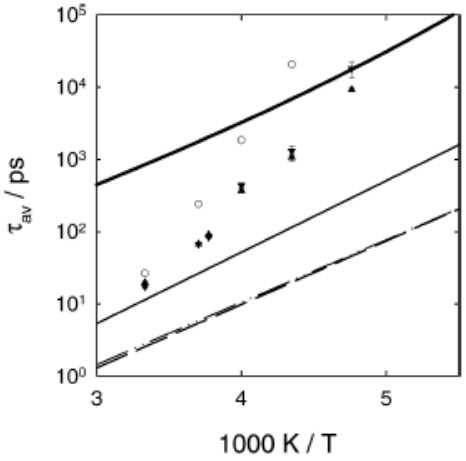

Inelastic neutron scattering study of a glass-forming liquid in soft confinement†

Zorn et al, Soft Matter 2008

INS-Examples

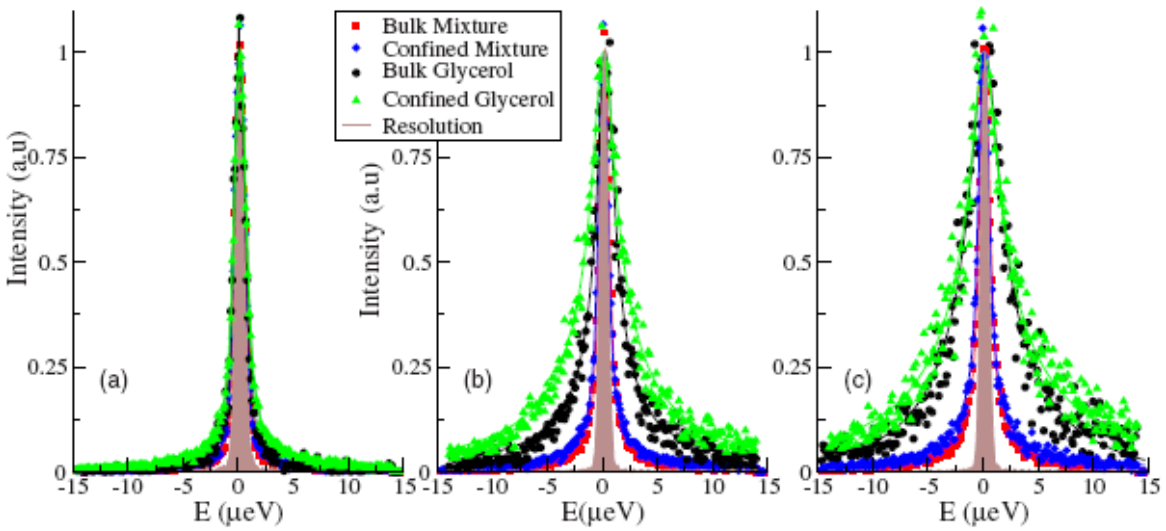

FIG. 3. (Color online) Incoherent quasielastic spectra of glycerol and the glycerol-trehalose solution in bulk and confined in porous silicon layers measured at T=310 K on the high resolution BS IN16. The intensity is corrected for empty sample contribution and normalized to maximum intensity. The displayed curves have been scaled to one at the maximum intensity for clarity. The resolution function of the apparatus is displayed as a filled gray shape. The solid lines are best fits of the data using a stretched exponential (see text). The graphs correspond to three different values of the transfer of momentum: (a) Q=0.54 Å^{-1}, (b) Q=0.96 Å^{-1}, and (c) Q=1.33 Å^{-1}.

Molecular dynamics of glycerol and glycerol-trehalose bioprotectant solutions nanoconfined in porous silicon

Bussellez et al JCP 2009

INS-Examples

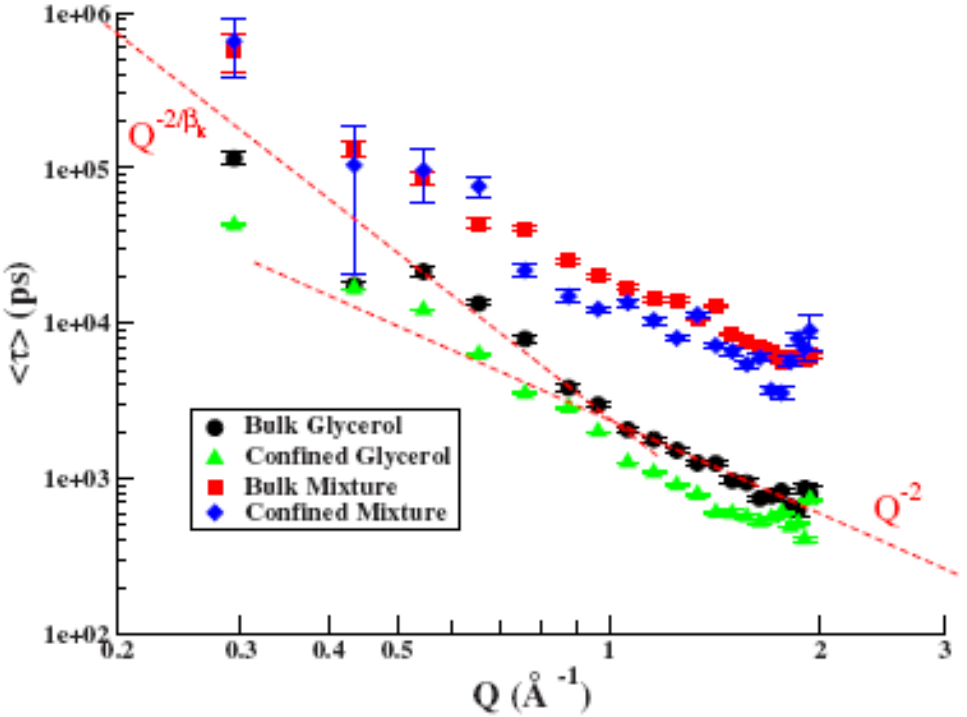

FIG. 4. (Color online) Average relaxation time $\langle\tau\rangle$ as a function of the transfer of momentum Q obtained from the incoherent quasielastic spectra at T=310 K for pure glycerol and the glycerol-trehalose solution in bulk and confined in porous silicon. Dashed lines superimposed on bulk glycerol data emphasize the crossover between two different power law variations.

Molecular dynamics of glycerol and glycerol-trehalose bioprotectant solutions nanoconfined in porous silicon

Bussellez et al JCP 2009